JOURNAL OF GEOPHYSICAL RESEARCH, VOL. 96, NO. B7, PAGES 11,849–11,864, JULY 10, 1991

The Equation of State of a Molten Komatiite 2. Application to Komatiite Petrogenesis and the Hadean Mantle

GREGORY H. MILLER,[1,2] EDWARD M. STOLPER, AND THOMAS J. AHRENS[1]

Division of Geological and Planetary Sciences, California Institute of Technology, Pasadena

New experimental data for the equation of state of a komatiitic liquid were used to model adiabatic melting in a peridotitic mantle. If komatiites are formed by >30% partial melting of a peridotitic mantle, then komatiites generated by adiabatic melting come from source regions that began their unmelted ascent in the lower transition zone (≈500-670 km) or the lower mantle (>670 km). The great depth of incipient melting implied by this model suggests that komatiitic liquids may form in a pressure regime where they are denser than their coexisting crystals, possibly the bulk mantle. Although komatiitic magmas are thought to separate from residual crystals in the mantle at a temperature ≈200°C greater than modern mid-ocean ridge basalts (MORBs), their ultimate sources are predicted to be diapirs that, if adiabatically decompressed from initially solid mantle, were more than 700°C hotter than the sources of MORBs and were derived from great depth. We also studied the evolution of an initially molten mantle, i.e., a magma ocean. Our model considers the thermal structure of the magma ocean, density constraints on crystal segregation, and approximate phase relationships for a nominally chondritic mantle. Crystallization will begin at the core-mantle boundary. Perovskite buoyancy at >70 GPa may lead to a compositionally stratified lower mantle with iron-enriched magnesiowüstite content increasing with depth. Large convective velocities in the magma ocean would prohibit crystal-liquid fractionation by settling or flotation until quiescent boundary layers form. Such boundary layers could form when the crystal content of the magma reaches a critical value (near 44 vol %) and, in the late stages of crystallization, around unmelted blocks of foundered protocrust. Matrix compaction and diapirism could also lead to fractionation effects. The upper mantle could be depleted or enriched in perovskite components relative to the bulk mantle. Olivine neutral buoyancy may lead to the formation of a dunite septum in the upper mantle, partitioning the ocean into upper and lower reservoirs, but this septum must be permeable.

1. INTRODUCTION

Miller et al. [this issue, hereafter referred to as M1] present new shock data for a molten komatiite composition and construct a complete PVT equation of state (EOS) by coupling our shock wave EOS with models for (1) the specific heat capacity, C_P or C_V, and (2) the thermodynamic Grüneisen parameter, $\gamma \equiv -\partial \ln T / \partial \ln V |_S$. Here, we use that thermodynamic model to investigate two problems of current petrologic interest: (1) the genesis of komatiitic liquids by adiabatic melting of mantle diapirs; and (2) the evolution of a deep, global magma reservoir.

The adiabatic melting of mantle diapirs has long been recognized as a probable mechanism for the generation of broadly basaltic liquids [*Verhoogen*, 1954]. A general parameterized model for this process has been formulated by *McKenzie and Bickle* [1988] and has been shown to be in qualitative agreement with a variety of observations. Komatiites may be formed by a similar process (but see *DeWit et al.* [1987]). For example, *Campbell et al.* [1989] suggested that komatiitic liquids are generated by diapirs that originate at the core/mantle boundary and note that this model can account for the spatial and temporal association of komatiites and tholeiites in Archaean greenstone belts. More recently, *Hess* [1990] has attempted to model quantitatively the adiabatic melting process for komatiites using assumed EOS data. In section 2 of this paper we combine our new EOS data and new phase relations [*Wei et al.*, 1990] to place constraints on the conditions necessary for the adiabatic formation of komatiitic liquids in a peridotitic mantle.

The high compressibility of liquid silicates suggests that ultrabasic liquids may be denser than some mantle mineral phases at high pressure [*Stolper et al.*, 1981]. *Agee and Walker* [1988*a*] estimated the pressure at which olivine would float in a komatiitic liquid, and used this information as part of a model for the evolution of an initially molten upper mantle [*Agee and Walker*, 1988*b*]. Other "magma ocean" scenarios have been postulated that incorporate the high density of ultrabasic magmas [*Nisbet and Walker*, 1982; *Ohtani*, 1985]. In section 3 we reexamine this problem from the perspective of our new data. This is posed as a problem of near-adiabatic crystallization and as such is complementary to the adiabatic melting problem investigated in section 2. It differs, however, in its sensitivity to the dynamical properties of the system (e.g., liquid viscosity and atmospheric heat flow). We will show that these dynamical factors may limit the extent of chemical fractionation in a molten Earth.

2. APPLICATION TO ADIABATIC MELTING AND KOMATIITE GENESIS

Adiabatic Gradients

The hypothesis that magma is generated during the adiabatic decompression of mantle rocks is based on the observation that temperature usually diminishes less with decreasing pressure in a totally solid system than it does along the anhydrous solidus of typical mantle rocks [*Verhoogen*, 1954]. An adiabatic diapir may consequently cross the solidus as it rises, thereby undergoing partial or complete fusion (Figure 1). Since the adiabatic gradient of a wholly molten system is solely a function of the EOS of the liquid and that of a partially molten system is a strong function of the liquid EOS, our komatiitic liquid EOS

[1] Also at Helen E. Lindhurst Laboratory of Experimental Geophysics, California Institute of Technology, Pasadena.

[2] Now at Department of Geology and Geophysics, University of California, Berkeley.

Paper number 91JB01203.
0148-0227/91/91JB-01203 $05.00

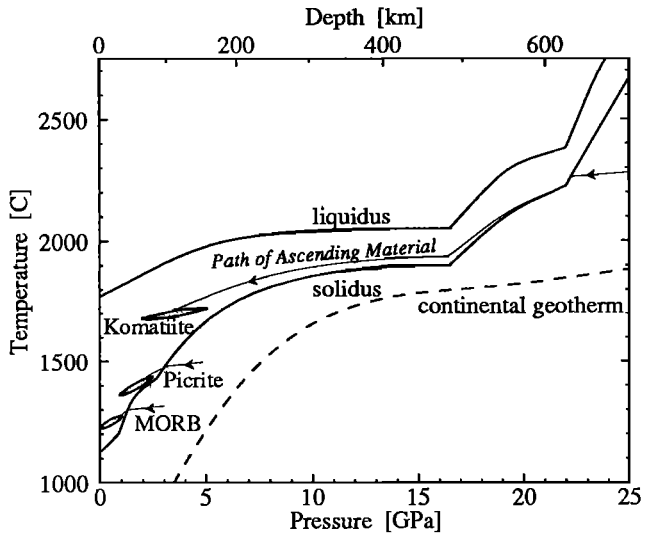

Fig. 1. Phase diagram for KLB-1 [*Takahashi*, 1986] with fields showing conditions under which komatiite [*Wei et al.*, 1990], MORB (as primitive melt) [*Presnall et al.*, 1979; *McKenzie and Bickle*, 1988], and picrite (also possible MORB parent) [*Green et al.*, 1979; *Elthon and Scarfe*, 1984] could have been extracted from their source regions. Adiabatic paths for ascending mantle source material, assuming single stage melting, are indicated by light lines. The komatiite field is based on the phase diagram of *Wei et al.* [1990] for a 25 wt % MgO komatiite. Komatiitic liquids with higher MgO content are anticipated to form under higher PT conditions [*Takahashi and Scarfe*, 1985; *Wei et al.*, 1990]. An estimate of the modern subcontinental mantle geotherm [*Mercier and Carter*, 1975; *Stacey*, 1975] is given by the bold dashed line. Changes in entropy associated with subsolidus reactions have been ignored.

provides a constraint on melting or crystallization under adiabatic conditions for ultrabasic systems. In this section, we develop a semiquantitative formulation of the adiabatic gradient in the melting interval of peridotite and consider its application to diapirism in the mantle and the genesis of komatiites. In this discussion we will equate adiabatic conditions with isentropic conditions.

Liquid komatiite adiabats may be calculated using the equation for the adiabatic gradient of a single, homogeneous phase in the absence of phase changes:

$$\left.\frac{\partial T}{\partial P}\right|_S = \frac{\alpha T}{\rho C_P} = \frac{\gamma T}{K_S}, \qquad (1)$$

where α is the volumetric thermal expansivity and ρ is the density. The high-pressure isentropic bulk modulus K_S can be determined as a function of pressure by differentiation of a Birch-Murnaghan isentropic EOS. For adiabats offset from the principal isentrope, K_S is determined from the principal isentrope and thermally corrected with a Mie-Grüneisen type term:

$$\left.\frac{\partial K_S}{\partial T}\right|_V = \gamma\rho C_V(1+\gamma-q), \qquad (2)$$

where $q \equiv \partial \ln\gamma/\partial \ln V|_S$. These adiabats can be constructed for molten komatiite with the experimentally determined EOS model presented earlier (M1). Molten komatiite adiabats are characterized by steep initial slopes but flatten substantially at high pressure (Figure 2). This flattening is due in part to the rapidly increasing bulk modulus and to a lesser extent to our assumption regarding γ:

$$\gamma = \gamma_0(V/V_0)^{q=1}. \qquad (3)$$

In a completely liquid system the adiabatic gradient is wholly specified by equation (1), given the liquid properties $\gamma_{liq}(P,T)$ and $K_{S\,liq}(P,T)$. Under subsolidus conditions, and in the absence of subsolidus reactions, the solid adiabat is also given by (1), evaluated with the thermodynamic properties appropriate to the crystalline assemblage. Upon crossing the solidus, however, the slope of the adiabat is modified by the entropy of fusion. To maintain adiabaticity, the temperature of the diapir must drop sufficiently to accommodate the entropy of fusion. The thermodynamics of this process have been described by *Carmichael et al.* [1974] for one-component systems and by *Rumble* [1976] for two-component systems. An analogous problem, that of condensation in a multi-component adiabatic atmosphere, has also been studied extensively [e.g., *Houghton*, 1977]. The meteorological term "wet adiabat" is used to describe the adiabat modified by a phase change, and we will adopt this term here to distinguish this case from the simple adiabat of equation (1).

We will approach this problem from the limit of complete melting where our data provide the most useful constraints. An expression for the adiabat can be derived by first writing the specific entropy of a magma consisting of crystals plus liquid:

$$S_{system} = (1-x)S_{liquid} + xS_{crystals} \qquad (4a)$$

$$S_{system} = S_{liquid} - x\Delta S, \qquad (4b)$$

where S_{liquid}, the specific entropy of the liquid, and ΔS, the instantaneous difference in specific entropy between the liquid and coexisting crystals, are functions of the liquid and crystal compositions at crystal mass fraction x and of temperature and pressure. Differentiating (4*b*) then leads to

$$dS_{system} \approx \left[\frac{C_P}{T} - \Delta S\left.\frac{\partial x}{\partial T}\right|_P\right]dT - \left[\alpha V - \Delta S\left.\frac{\partial x}{\partial T}\right|_P\left.\frac{\partial T}{\partial P}\right|_x\right]dP, \qquad (5)$$

where C_P, V (the specific volume), and α are thermodynamic properties of the liquid. We have made the approximation that ΔS is constant, which will be taken to be approximately 1.0 R/mol(atoms) [*Stishov*, 1969, 1988; *Jeanloz*, 1985] and independent of liquid composition and the crystallizing species. Experi-

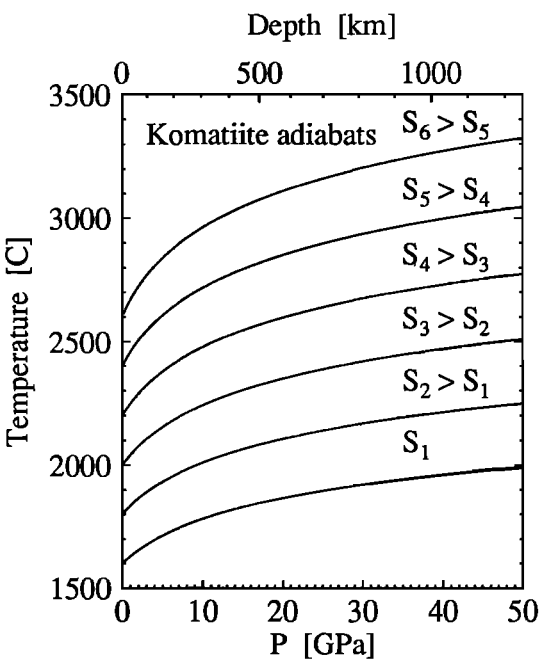

Fig. 2. Several adiabats for liquid komatiite (M1).

mental determinations of the entropy of fusion, ΔS_f (note that $\Delta S_f \neq \Delta S$ in general), for silicates at 1 bar indicate that the first of these approximations is good to better than a few percent for simple ultrabasic systems ($\Delta S_f/R$ is 1.03 for fayalite, 1.01 for enstatite, 1.00 for diopside at their respective 1-bar melting temperatures [*Stebbins et al.*, 1984]). In a complex liquid the entropy is given by the sum of the entropies of its components and an additional term arising from the permutability of the mixture. This latter term is always positive; hence the entropy of fusion of a multicomponent phase or assemblage will always be greater than ΔS_f for a simple mineral end-member. For complex crystalline phases, site mixing also contributes a permutability term to the solid entropy, and there is an analogous contribution to the entropy of fusion but with opposite sign. We anticipate that the greater permutability of the liquid will always favor $\Delta S_f > R$ for ultrabasic systems. The average entropy difference between a wholly molten mantle and a wholly crystalline mantle (at constant T and P) will, therefore, almost certainly be greater than 1.0 R/mol(atoms). The specific entropies per atom of several components of mantle phases (forsterite, enstatite, diopside, jadeite, pyrope, and Tschermack's pyroxene) are all quite similar [*Robie et al.*, 1978]. They differ from one another by less than R/4; thus the instantaneous entropy difference between liquid and coexisting solid (ΔS in equation (4)) will probably be $\geq R$ as well. The assumption that ΔS has a constant value of 1.0 R/mol(atoms) will probably, therefore, lead to an underestimation of the average difference between ultrabasic liquid and crystal entropies. This will lead to conservative conclusions, as will be demonstrated, so we will adopt it for purposes of illustration.

Setting $dS_{system} = 0$ in (5), we obtain the slope of the wet adiabat:

$$\left.\frac{\partial T}{\partial P}\right|_{S,\,T_{liquidus}\geq T\geq T_{solidus}} \approx \frac{\left[\frac{\gamma T}{K_S}\right]_{liq} - \frac{T\Delta S}{C_{P\,liq}}\left.\frac{\partial x}{\partial T}\right|_P \left.\frac{\partial T}{\partial P}\right|_x}{1-\frac{T\Delta S}{C_{P\,liq}}\left.\frac{\partial x}{\partial T}\right|_P}. \quad (6)$$

The first term in the numerator is the adiabatic gradient of the crystal-free liquid. Note that when the slope of the constant x contour ($\partial T/\partial P|_x$) is equal to the slope of the crystal-free adiabat ($\partial T/\partial P|_{S,x=0} \equiv \gamma T/K_S$), the wet adiabat will have this same slope. For a given value of ΔS, the greater the angle in PT space at which the liquidus and solidus intersect the liquid adiabat, the more rapidly (in terms of pressure or depth) the wet adiabat will cross through the melting interval. The liquidus and solidus for the Earth's deep upper mantle are believed to be nearly flat [e.g., *Scarfe and Takahashi*, 1986]. Since the adiabats for komatiitic liquids are also nearly flat in this interval (Figure 2), we predict that the melt fraction of diapirs will change little through this pressure interval.

Rigorous evaluation of $\partial x/\partial T|_P$ and $\partial T/\partial P|_x$ requires detailed knowledge of the Gibbs free energy surfaces of the liquid and crystalline phases [*Rumble*, 1976]. We can make several generalizations without evaluating these terms, however. Adiabats can be constructed for the liquid at all pressures (Figure 2), and similar curves can be calculated for the crystalline assemblage at these same values of specific entropy. Since the specific entropy of the solid is always less than that of the liquid at a given temperature and pressure, the solid isentrope must always be at higher temperature (Figure 3). Note that where phases and assemblages described by the isentropes shown in Figure 3 are metastable the isentropes are shown as lighter curves. The wet adiabat connects the liquid adiabat at its intersection with the liquidus to the solid adiabat at its intersection with the solidus. While the shape of this wet adiabat will depend on the thermodynamics of the phase transition, its intersections at the solidus and liquidus are uniquely specified by knowing the all-liquid and all-solid adiabats (for the same value of specific entropy) and the liquidus and solidus. The points of incipient melting and incipient crystallization under adiabatic conditions can therefore be determined without knowledge of the function x(T,P).

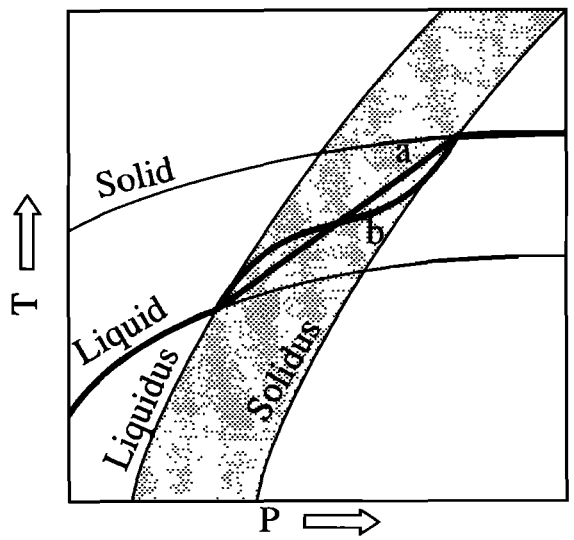

Fig. 3. Cartoon showing that the points of incipient melting and incipient crystallization under adiabatic conditions are determined uniquely by the all-liquid and all-solid adiabats and by the liquidus and solidus. Since the solid has an intrinsically lower specific entropy at constant T and P, it must be hotter than the liquid to have the same specific entropy. The intersection of the liquid adiabat with the liquidus is the point of incipient crystallization, and the intersection of the solid adiabat with the solidus is the point of incipient melting. These intersection points are joined in the two-phase region by the wet adiabat whose shape is a complex function of the Gibbs free energy surfaces. Two possible wet adiabats have been drawn. The straight line a corresponds approximately to the case where crystallinity varies linearly with temperature. The curved wet adiabat b corresponds to the case where crystallinity changes rapidly near the liquidus and solidus but more slowly in between.

On isobaric melting, the thermal energy of the solid ($C_P\,dT \approx 3R\,dT$) is applied to the latent heat of fusion ($T\Delta S\,dx \approx TR\,dx$). Equating these terms and integrating, we find that for a solid and liquid of the same composition to have the same specific entropy at a given pressure, the solid must be hotter than the liquid by $\Delta T \approx (e^{1/3}-1)T_{liquidus} \approx 0.4T_{liquidus}$, or about 800 K in the upper mantle. To the degree that we have underestimated the entropy of fusion by ignoring the permutability of the liquid, we may have also underestimated this change in temperature. Thus, for a solid diapir to melt completely upon adiabatic decompression, its initial temperature would have to be at least 800 K greater than that of the emergent liquid. The probable phase diagrams for typical peridotitic or chondritic compositions (discussed later) preclude this possibility for solid diapirs that begin to melt in the upper mantle, because the high-pressure solidus is not 800 K hotter than the low-pressure liquidus anywhere in the pressure range of the upper mantle and transition zone. Consequently, the only way that adiabatic diapirs could become significantly molten (≥50 wt %) in the upper mantle is if they originate in the transition zone or lower

mantle or if they were already partially molten (e.g., by heating at a boundary layer) when adiabatic ascent within the upper mantle was initiated.

In order to understand the qualitative features of an adiabatic system in the melting interval, it is necessary to evaluate $\partial x/\partial T|_P$. A crude estimate of the degree of crystallinity can be made by assuming the crystal mass fraction varies linearly with temperature at constant pressure:

$$x \approx \frac{T_{liquidus}-T}{T_{liquidus}-T_{solidus}} \quad (7)$$

for $T_{liquidus} \geq T \geq T_{solidus}$. Alternatively, *McKenzie and Bickle* [1988] showed that a cubic polynomial appears to provide a good pressure-independent fit to a variety of experimental x(T) measurements in peridotite systems at low pressure. There are reasons to doubt that either of these functions accurately describes the details of crystallization, particularly at high pressure (>10 GPa). However, the general features of the resulting calculations are similar regardless of which function is employed, so at least those aspects of the calculations that are not sensitive to the details of x(T) can be evaluated. Again we emphasize that this function only governs the behavior of the adiabat within the melting interval. For a particular value of specific entropy, all calculated adiabats will converge at the liquidus and solidus intersection points (Figure 3) regardless of the x(T) function used.

A phase diagram for an upper mantle comprised of fertile peridotite has been schematically constructed (Figure 4) from the high-pressure experiments of *Takahashi and Scarfe* [1985], *Takahashi* [1986], and *Ito and Takahashi* [1987] on the KLB-1 spinel lherzolite (this xenolith, from Kilbourne Hole, New Mexico, is considered a reasonable analog for a peridotitic mantle [e.g., *Takahashi and Scarfe*, 1985]). The mantle liquidus rises sharply at low pressure but flattens significantly near ≈12 GPa and may even have a maximum [*Scarfe and Takahashi*, 1986]. With increasing pressure to ≈15 GPa, the melting interval ($T_{liquidus}-T_{solidus}$) also probably decreases [*Herzberg*, 1983].

Adiabats that go through the melting interval have been constructed for the two x(T) functions and are shown in Figure 4. The extent of melting is shown in Figure 5 for the two calculations. We used the adiabats of our komatiite to represent those of the liquid, independent of the extent of fusion, since attempts to account for chemical variation (through addition or subtraction of olivine components) yield similar results. The crystal-free adiabats have roughly the same slope as the liquidus in the 250-450 km interval of the upper mantle, so the degree of crystallinity of rising diapirs would not vary rapidly with pressure in this region of the upper mantle (Figure 5) (In fact, as shown in Figure 5, the degree of melting actually decreases with pressure in this interval; we attach no significance to this as it is very sensitive to the specific liquidus and solidus slopes that are chosen.) In no case does an adiabat cross from below the solidus to the liquidus over the pressure interval of the upper mantle (including the transition zone), so as pointed out above, adiabatic diapirs with very large degrees of partial melting would have to originate in the transition zone or lower mantle. If the permutability contribution to the entropy of fusion were properly accounted for, the depth of incipient melting would be even greater for a given degree of partial melting. With a linear x(T) model, melting is distributed evenly between the liquidus and solidus. With the *McKenzie and Bickle* [1988] parameterization, crystallinity varies rapidly near the solidus and liquidus but more slowly in between. The adiabats are consequently

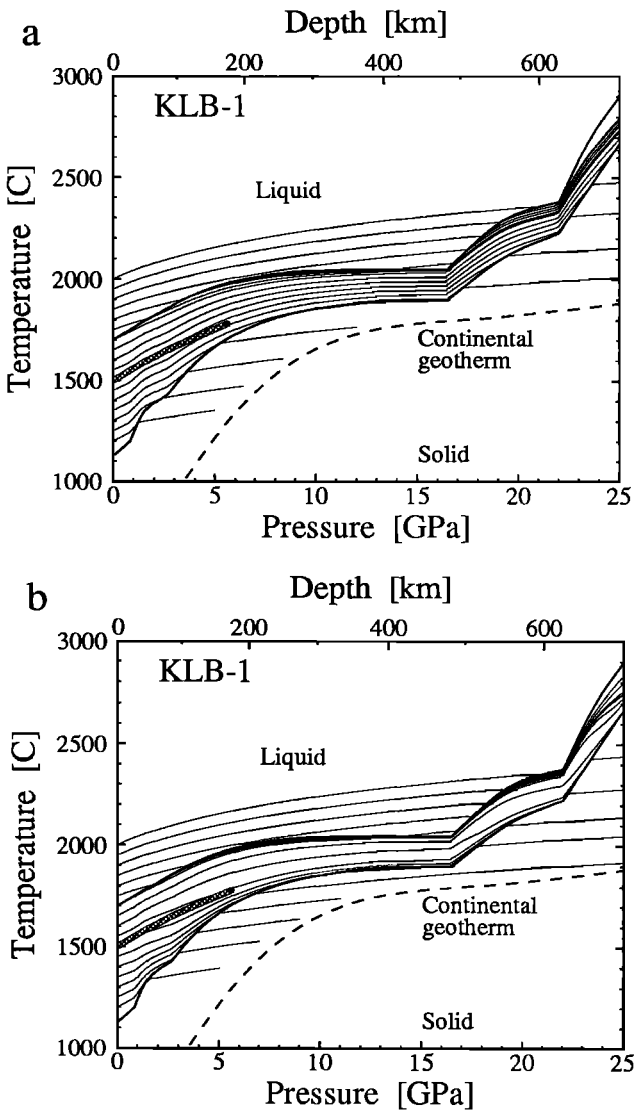

Fig. 4. Model phase diagrams for the upper mantle with superimposed adiabats: (*a*) linear x(T) relationship, and (*b*) cubic x(T) relationship from *McKenzie and Bickle* [1988]. Adiabats are calculated at 50° intervals (at P=0) in each case. The circle represents the olivine ± clinopyroxene ± garnet liquidus cosaturation point for a komatiite broadly similar to the sample we studied [*Wei et al.*, 1990]. The stippled band is the trace of the komatiite liquidus.

nearly tangential to the solidus and liquidus curves. With the linear model, up to 45% partial melting is possible if a diapir crossed the solidus at the base of the upper mantle (400 km). Only 40% melting is possible with the parameterization of *McKenzie and Bickle* [1988] under the same conditions.

In the 0-5 GPa range our calculations predict degrees of partial melting similar to the calculation of *McKenzie and Bickle* [1988]. We predict melt fractions about 20% less than their model (comparing our Figure 5*b* with Figure 7*a* of *McKenzie and Bickle* [1988]). This small difference can be attributed in part to different assumptions regarding ΔS; their model implies a value of about 0.63R. In order to generate the amount of melt they consider to be typical of mid-ocean ridge basalt (MORB) (10-15%), we require that the mantle be at least 100° hotter than the 1280°C potential temperature (defined as the temperature a mantle parcel would have at 1 bar if it were adiabatically decompressed as a metastable solid) that they advocate.

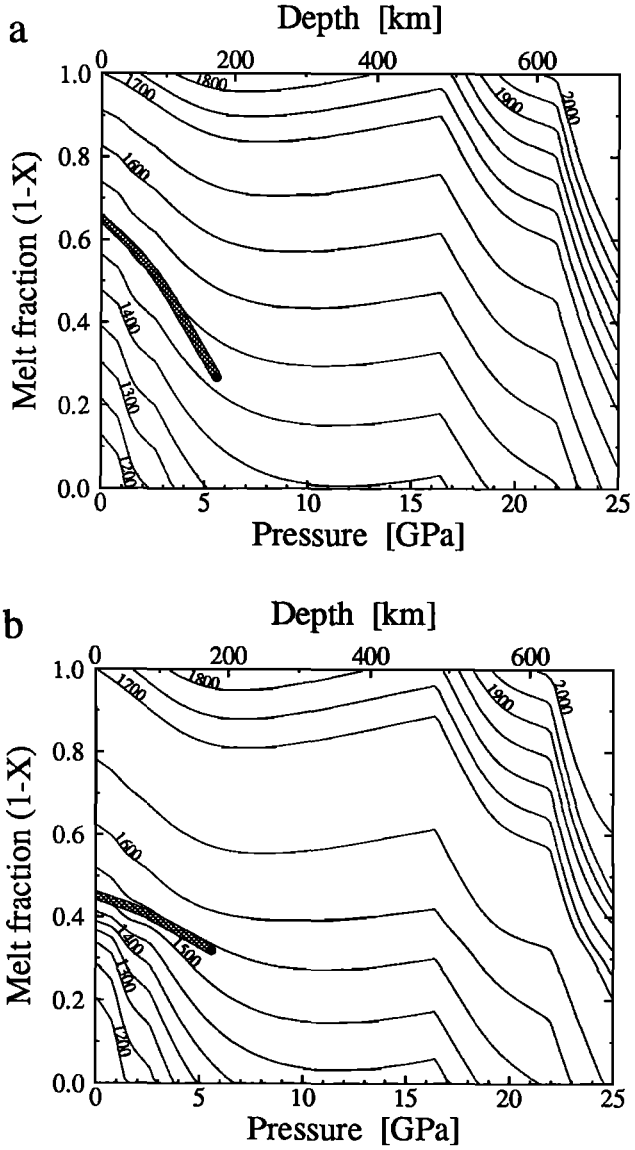

Fig. 5. Weight fraction of liquid generated under adiabatic conditions for (*a*) linear x(T) model, and (*b*) *McKenzie and Bickle* [1988] x(T) parameterization. Each curve represents a single adiabat. The numbers on the curves represent the final 1 bar temperatures of the partially molten diapirs (in degrees Celsius). These curves are the Px projections of the PT adiabats in Figure 4. The circle represents the point of olivine ± clinopyroxene ± garnet cosaturation on a komatiite liquidus [*Wei et al.*, 1990], and the stippled band is the projection of the trace of the komatiite liquidus. Note that melt fractions do not vary significantly in the lower 200 km of the upper mantle.

Diapiric Origin of Komatiites

Wei et al. [1990] determined the phase diagram for a komatiite of broadly similar composition to the one we have studied. This phase diagram is superimposed on the KLB-1 phase diagram (Figure 4) in Figure 6. *Wei et al.* [1990] suggest that this komatiite could have separated from either an olivine ± clinopyroxene ± garnet residue at 5.6 GPa and 1780°C, or an olivine residue at lower pressure and temperature. The olivine ± clinopyroxene ± garnet cosaturation point for this komatiite is within ≈10°C of the maximum temperature at which olivine + clinopyroxene ± garnet saturated liquids can be generated by melting of KLB-1 at 5.6 GPa, so the phase equilibria are roughly compatible with the idea that a komatiitic liquid of this composition could have been segregated from a KLB-1-like source under these conditions. We calculate that a KLB-1-like source would consist of 27-32% partial melt at 5.6 GPa and 1780°C, which, although dependent on the specific form of the x(T) functions we have used, is compatible with the 10-30% partial melting of a KLB-1-like source we calculate by mass balance of the *Wei et al.* [1990] data. If komatiitic liquids were generated by 10-30% partial melting of adiabatic KLB-1-like diapirs at 5.6 GPa, then our calculations suggest that the source region of the diapirs (provided they were initially unmelted) would have to be in the 10-20 GPa range and that they would have begun to melt between 10 GPa, 1850°C (10%) and 20 GPa, 2150°C (30%). Whether the melt fraction is 10% or 30% makes such a big difference in the minimum depth because melt fraction does not change significantly in the ≈8-16 GPa (≈250-450 km) interval; melt fractions greater than ≈15% require that melting commence in the transition zone.

The *Wei et al.* [1990] phase relations for komatiite and those for KLB-1 peridotite are also compatible with segregation of komatiitic liquid from olivine-only residues at pressures lower than 5.6 GPa, implying >30% partial melting. Estimates of the degree of partial melting of peridotite required to generate komatiitic liquid plus residual olivine [e.g., *Arndt*, 1977] are typically of the order of 50-80%. In order to reconcile such high melt fractions with the results of our calculations and the komatiite liquidus given by *Wei et al.* [1990], the komatiitic liquid would have to separate from its olivine residue at pressures less than 3 GPa (i.e., the adiabat in Figure 4*a* that intersects the Wei et al. liquidus at 3 GPa is 50% molten at this point; the maximum melt fraction obtained with the *McKenzie and Bickle* [1988] x(T) function is about 45% at 1 bar). Subso-

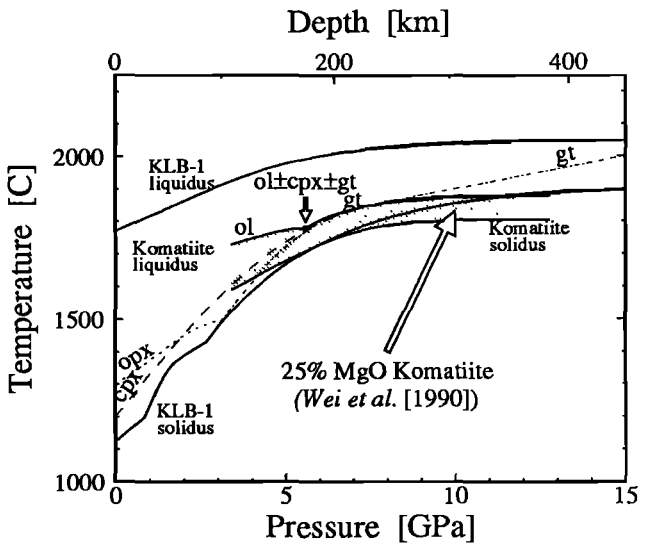

Fig. 6. Liquidus and solidus for a 25 wt % MgO komatiite determined by *Wei et al.* [1990]. This komatiite is similar in composition to the one we have studied. This phase diagram is superimposed upon the phase diagram for mantle peridotite (KLB-1 [*Takahashi*, 1986]). The appearance of garnet (gt), clinopyroxene (cpx) and orthopyroxene (opx) are shown for the peridotite as dashed lines. Olivine is the liquidus phase of the KLB-1 peridotite. Liquidus appearance of olivine, clinopyroxene, and garnet are indicated on the komatiite liquidus. If this komatiite were formed by the partial fusion of peridotite, then the komatiite would have segregated from residual olivine at pressures less than 5.2 GPa. Higher pressures lead to inconsistencies between the peridotite and komatiite phase equilibria.

lidus diapirs that could generate these degrees of partial melting would have to originate in the transition zone or deeper ($P \geq 21$ GPa) with temperatures greater than 2180°C.

If crystal-liquid segregation is possible in ascending diapirs, then it may be possible to fractionate dense crystalline phases, such as garnet-majorite, from komatiitic liquids. Olivine is buoyant in komatiitic liquids at pressures greater than ≈9 GPa, but garnet-majorite is buoyant in komatiitic liquids only at pressures greater than about 19 GPa (M1). Mechanisms by which garnet-majorite fractionation could occur in the source diapirs of komatiites at the relatively low melt fractions expected based on our calculations at pressures greater than 5.6 GPa are not certain, but garnet-majorite fractionation trends have been inferred for some South African peridotites [*Herzberg et al.*, 1988], and several authors [e.g., *Green*, 1975; *Nesbitt et al.*, 1979; *Jahn et al.*, 1982; *Ohtani*, 1984] have suggested that garnet fractionation may have been important in the genesis of so-called aluminum-depleted komatiites. We note in particular the suggestion of *Ohtani* [1984] that the diapirs that generate Al-depleted komatiites originate deeper in the mantle than those that generate Al-undepleted komatiites. As a consequence of their deeper origin, they would achieve higher degrees of partial melting, which could facilitate garnet fractionation, perhaps aided by the contrasting buoyancy of olivine/pyroxene and garnet in ultrabasic liquids at the relevant pressures. It can be seen in Figures 4 and 5 that small differences in source pressure and temperature at depths >500 km can lead to large differences in melt fraction in the 17-25 GPa pressure interval because the KLB-1 solidus and liquidus are steep compared to the all-liquid adiabats in this region; for example, increasing the source temperature by about 50° at 500 km would change the melt fraction by about 5%, and the effect is even larger at lower pressures. Consequently, small differences in source temperature at these depths could control whether the melt fraction is large enough (at high pressure) to facilitate garnet-majorite fractionation (Al-depleted) or not (Al-undepleted).

Several authors have suggested that komatiitic liquids could be generated by pseudoinvariant melting of peridotites at high pressures [*Takahashi and Scarfe*, 1985; *Herzberg and O'Hara*, 1985; *O'Hara et al.*, 1975]. *Takahashi and Scarfe* [1985] reported the formation of a komatiitic liquid as the initial melt of KLB-1 near 1800°C and 5-7 GPa, although the melt fractions were not determined and may have been large given that solid-liquid segregation occurred within their charges. In a similar experiment by *Takahashi* [1986], also on KLB-1, where both liquid and crystal compositions were reported, a komatiitic liquid generated at 5 GPa and 1700°C (run 53) represents over 60% partial melting according to mass balance calculations. Thus, it is not clear that these experiments provide support for the pseudoinvariant melting hypothesis. In any case, if komatiitic liquids can indeed be generated by small degrees of partial melting in the 5-7 GPa pressure range, they must differ from the one studied by *Wei et al.* [1990] if the phase relationships shown in Figure 6 are accurate, because the *Wei et al.* [1990] komatiite liquidus is some 100° higher than the KLB-1 solidus in this pressure range and its solidus is also higher than the KLB-1 solidus.

In summary, our calculations suggest that mechanisms for komatiite genesis that call for large (>30%) degrees of partial melting at $P < 5$-6 GPa by adiabatic decompression require diapirs that begin to melt in the transition zone or deeper at pressures in excess of 20 GPa. Mantle potential temperatures in excess of 1750°C are required. Unless these source regions were anomalously hot with respect to the bulk mantle, the entire Archean upper mantle would have been partially molten [*Cawthorn*, 1975], and magmatic activity originating in the mantle would overwhelmingly be controlled by this widely distributed komatiitic melt. However, the juxtaposition of distinct tholeiitic and komatiitic magma types in Archean terrains, which cannot simply be related by low pressure crystal fractionation, suggests a nonuniform upper mantle thermal regime in the Archean. Thus, komatiites might represent melts extracted from hotter than average upper mantle, generated, for example, in deep thermal boundary layers. Thermal boundary layers that could generate such anomalously hot diapirs could have been located between the upper mantle and transition zone [*Anderson*, 1984, 1989], between the transition zone and lower mantle [*Jeanloz and Richter*, 1979; *Lees et al.*, 1983; *Jeanloz and Knittle*, 1989], or even at the core-mantle boundary [*Jarvis and Campbell*, 1983]. If komatiites can be formed by small degrees (e.g., <15%) of partial melting, then more modest potential temperatures (1700-1750°C) would be allowed. If komatiitic liquids can be formed as initial melts in the 5-7 GPa pressure range, then potential temperatures even as low as 1600°C are possible. Pyroxene geothermometry indicates that the potential temperature of the mantle beneath continents is about 1600°C [*Mercier and Carter*, 1975], so if this latter view of the conditions required for production of komatiitic liquids is valid, it should be possible to generate komatiitic liquids in the modern mantle. To the extent that modern magmas approaching komatiites are uncommon (although some paleogene "picritic" magmas get close to "komatiitic" in composition [*Ganisser et al.*, 1979; *Echeverria*, 1982]), this suggests to us that models invoking low degrees of partial melting, including those involving pseodoinvariant melting, are unlikely to be correct.

Figure 1 compares the conditions that have been suggested for the formation of komatiitic liquids to those that have been suggested for the genesis of primary magmas parental to modern MORBs (*Presnall et al.* [1979] versus *Green et al.* [1979] and *Elthon and Scarfe* [1984]). Note that we have restricted our discussion to a KLB-1 model for mantle source material and that the quantitative details will vary with the phase equilibria of the potential source. Thus, for example, more fertile source materials will have lower solidi, thereby allowing greater degrees of melting for a given potential temperature, but depleted sources will have higher solidi and require higher temperatures. The most surprising result of our analysis is that although the temperatures of melt segregation for komatiitic liquids implied by scenarios that suggest >30% partial melting are only ≈200°C higher than those of modern MORBs, the configuration of the solidus and liquidus of likely source peridotites requires their ultimate sources to be diapirs that, if adiabatically decompressed from initially solid mantle, were more that 700°C hotter than the sources of MORBs and derived from great depth in the mantle.

3. Application to a Magma Ocean and the Evolution of the Hadean Mantle

Many independent arguments suggest that it is plausible that at least the upper mantle of the Earth was substantially molten in the Hadean. This melting could have resulted from the accretion of the Earth [*Kaula*, 1979; *Abe and Matsui*, 1986; *Matsui and Abe*, 1986; *Zahnle et al.*, 1988; *Ahrens*, 1990; *Agee*, 1990], core formation [*Birch*, 1965; *Solomon*, 1978; *Shaw*, 1979], the impact formation of the moon [*Benz et al.*, 1986, 1987; *Cam-*

eron and Benz, 1989; *Stevenson*, 1989], or from some combination of these mechanisms. Recognition of this possibly molten state, together with the idea that ultrabasic liquids may be denser than olivine and other silicate phases at relatively shallow mantle depths, has prompted speculation on the evolution of the upper mantle from a magma ocean [*Nisbet and Walker*, 1982; *Ohtani*, 1985; *Agee and Walker*, 1988*b*]. The liquidus topologies of several ultrabasic systems including iron-depleted C1 meteorite [*Ohtani et al.*, 1986; *Ohtani and Sawamoto*, 1987], peridotite [*Takahashi and Scarfe*, 1985; *Scarfe and Takahashi*, 1986; *Ito and Takahashi*, 1987], komatiite [*Bickle et al.*, 1977; *Wei et al.*, 1990], and perovskite [*Heinz and Jeanloz*, 1987; *Knittle and Jeanloz*, 1989] provide critical constraints on this evolution. Our new data on the equation of state of molten komatiite provide further constraints and allow for more quantitative modeling than was previously possible. In this section we consider applications of the equation of state of a komatiitic liquid to the evolution of the Hadean mantle from an initial wholly molten state.

The following discussions will focus on EOS constraints on the evolution of a molten mantle, but many of these constraints cannot be properly evaluated without fluid dynamical considerations. Density contrasts govern whether a crystal would rise or sink in a quiescent liquid, but viscosities, convection velocities, and cooling rates are equally important in determining the ultimate fate of crystals in a convecting magma system. Accordingly, an effort will be made to understand the fluid dynamics of such a system as it evolves.

We will assume that the entire mantle was molten and that the undifferentiated mantle had an iron-depleted C1 composition [*Agee and Walker*, 1988*b*]. For simplicity, we will henceforth refer to this iron-depleted C1 composition simply as C1. Because the mantle is assumed to be liquid and would have low viscosity, we will also assume that the thermal state of the mantle was approximately adiabatic. As the Earth cools, boundary layers may develop, and crystal segregation may occur. Both of these circumstances would make the system nonadiabatic, at least on local length scales. These special circumstances may play important roles in the evolution of the Earth, as will be discussed below. Furthermore, although convection requires some degree of superadiabaticity, we will adopt the adiabatic state as a reference state and follow its development with time.

An approximate fit to the major element chemistry of C1 can be obtained from a mixture of olivine (20.4 wt % of $Fo_{0.98}Fa_{0.02}$), pyroxene (38.1 wt % of $En_{0.9}Fs_{0.1}$), and komatiite (M1) (41.5 wt %). From the assumption that liquids mix ideally with respect to volume (i.e., $V=\sum x_i V_i$, where V_i is the specific volume of a liquid with the composition of component i and x_i is its mole fraction in the mixture) we can derive the adiabatic gradient of a liquid of C1 composition:

$$\left[\frac{\gamma T}{K_S}\right]_{mixture} = \frac{\sum_i \left[\frac{x_i V_i C_{Vi}}{V_i K_{Si} - \gamma_i^2 T C_{Vi}} (\gamma_i T)\right]}{\sum_i \left[\frac{x_i V_i C_{Vi}}{V_i K_{Si} - \gamma_i^2 T C_{Vi}} (K_{Si})\right]}, \quad (8)$$

where K_{Si} is the isentropic bulk modulus of a liquid with the composition of component i, C_{Vi} its constant volume heat capacity, and γ_i its Grüneisen parameter. The high-pressure, high-temperature thermodynamic parameters for each liquid end-member (V_i, K_{Si}, and γ_i) are calculated from a Birch-Murnaghan EOS (equations (19) and (27) and Table 5 in M1) with Mie-Grüneisen thermal corrections for the pressure (M1, equation (28)) and bulk modulus (equation (2)). C_V is taken as 3R and $q=1$ for each component; both C_V and γ are assumed independent of temperature.

The phase diagram for an iron-depleted C1 upper mantle has been investigated by *Ohtani et al.* [1986] and *Ohtani and Sawamoto* [1987] and a modified version is shown in Figure 8. The diagram is largely schematic at P>25 GPa but was estimated as follows. Under lower mantle conditions we expect a dominantly perovskite+magnesiowüstite subsolidus mineralogy. A schematic phase diagram for such a system at 100 GPa has been constructed (Figure 7) assuming ideal mixing of liquid components using the data of *Knittle and Jeanloz* [1989] as an upper bound for perovskite melting and the calculations of *Ohtani* [1983] for magnesiowüstite. On the basis of this model calculation we expect that perovskite will be the liquidus phase throughout the lower mantle and the P-T diagram shown in Figure 8 incorporates this result.

Several adiabatic contours for the partially molten mantle are superimposed on a model C1 phase diagram in Figure 8. The wet (crystal+liquid) adiabats are calculated as discussed in section 2, with crystal content varying linearly with temperature at constant pressure. Two general conclusions can be drawn from Figure 8 that are not sensitive to its detailed topology. First, crystallization of a wholly molten mantle would begin near the core-mantle boundary (Figure 8). Second, if the upper mantle (i.e., P<21 GPa) were wholly molten and the entire mantle were adiabatic, then the lower mantle could be at least partially molten to great depth [cf. *Agee and Walker*, 1988*b*]. For example, if the mantle were wholly molten to >30 GPa, then our calcula-

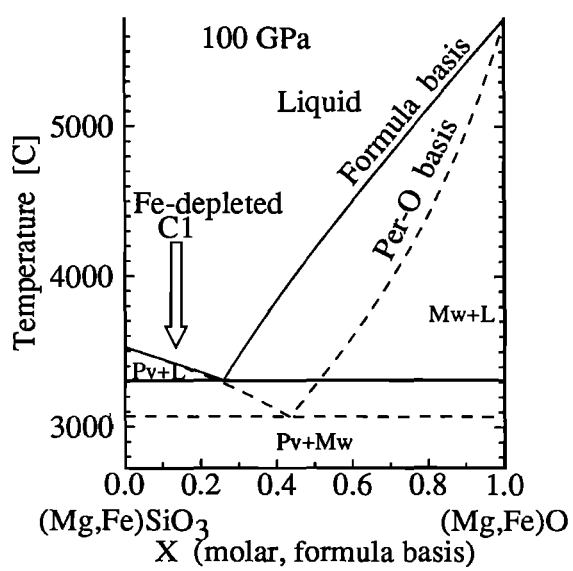

Fig. 7. Approximate phase diagram for a chondritic lower mantle at 1 Mbar. The approximate melting temperature of $Mg_{0.9}Fe_{0.1}SiO_3$ perovskite is 3800 K [*Knittle and Jeanloz*, 1989] and that of $Mg_{0.6}Fe_{0.4}O$ magnesiowüstite is calculated to be ≈6000 K [*Ohtani*, 1983]. The phase diagram was calculated by assuming that ΔS_f is R/mol(atoms) for each phase with a simple solution model. The solid diagram assumes that the molecular species in the melt phase are given by the mineral formula. The dashed curve assumes one molecular species per oxygen atom and has been converted to the formula basis in the figure. The arrow indicates the approximate bulk composition of a chondritic mantle. For both models, perovskite will be the liquidus phase at ≈3900 K. The solidus is at 3580 K with the formula basis and 3340 K with the oxygen basis.

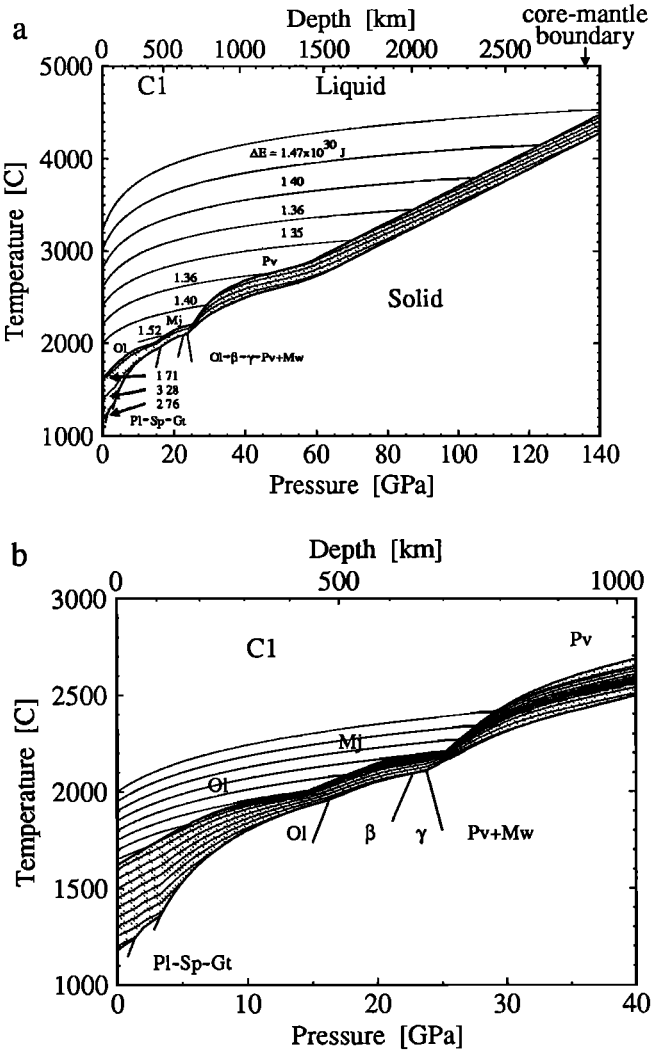

Fig. 8. Estimated C1 phase diagram for the mantle compiled from experimental data of *Heinz and Jeanloz* [1987], *Ito and Takahashi* [1987], *Knittle and Jeanloz* [1989], *Ohtani et al.* [1986], *Ohtani and Sawamoto* [1987], *Scarfe and Takahashi* [1986], and *Takahashi* [1986]. Beyond 25 GPa this phase diagram is highly schematic and based solely on the perovskite liquidus (see Figure 7). The liquidus phases are olivine to ≈15 GPa followed by garnet-majorite to ≈25 GPa and perovskite at higher pressures. Subsolidus reaction boundaries for the sequence plagioclase→spinel→garnet and olivine→β modified spinel→γ spinel→perovskite + magnesiowüstite are also indicated. Superimposed on the phase diagram (Figure 8*a*) are adiabatic contours. The entropy of fusion causes subliquidus adiabats to remain in the melting interval over extensive depth intervals. Note that crystallization will begin at the base of a whole Earth magma ocean. The actual temperature profile of a magma ocean will differ from the adiabatic contours wherever boundary layers develop. These boundary layers may form in the lower mantle because of viscosity contrasts, in the upper mantle because of olivine neutral buoyancy, and at the surface where an itinerant crust may form. The difference in energy (in 10^{30} J) between a given wet adiabat and the one above it is written on the adiabat curves. At high temperatures the curves are at $\approx 1.4 \times 10^{30}$ J intervals. At lower temperatures the energy difference increases. Figure 8*b* is an enlargement of Figure 8*a*, emphasizing the upper mantle and transition zone. Contours in this figure are at 50° intervals at P=0.

tions suggest that the zone of partial fusion could extend to the core-mantle boundary (under adiabatic conditions). An adiabatic mantle would therefore not have a crystalline floor initially but rather would have a partially molten zone extending to the core. This can be seen by following the adiabats, which, as described in section 2, are slow to traverse the melting interval. This conclusion is independent of the details of crystallization (i.e., no knowledge of $\partial T/\partial P|_x$ and $\partial x/\partial T|_P$ is required) but is, of course, sensitive to our assumed lower mantle liquidus and solidus.

If any chemical fractionation (e.g., crystal-liquid segregation) occurs, the phase relations and adiabatic contours described above will not be strictly applicable to the residual liquid. In the following sections we use this model C1 system as an approximation to fractionated systems as well. A more rigorous analysis is not justified given available phase equilibrium data.

Time Scale for Cooling of a Terrestrial Magma Ocean

Although the lifetime of a magma ocean is not of direct concern to us here, the extent of chemical fractionations may be limited by the rate at which the mantle cools [*Melosh and Tonks*, 1989; *Tonks and Melosh*, 1990]. For example, in the absence of any atmosphere and crust, the planet might cool so rapidly that little differentiation is possible. At the other extreme, if we allowed an arbitrarily long cooling time, then the molten Earth would be quiescent (nonconvecting) and could evolve through fractional crystallization to give a strongly layered body. Accordingly, in this section, we attempt to estimate the rate of heat loss from the molten Earth. The heat flux from the molten Earth will depend on the surface temperature and on the opacity of the atmosphere, while the surface temperature depends on whether or not a crust could form. In the following subsection we discuss the importance of an atmosphere and arrive at an approximation for the heat flux as a function of surface temperature. In the subsequent subsection we consider whether or not a crust could form if the upper mantle were a superheated liquid and what influence this might have on the heat flux from the magma ocean.

Heat flow through the atmosphere. The ability of a protoatmosphere to transmit heat from a magma ocean is strongly dependent on the chemical constitution of the atmosphere. The chemical composition of a protoatmosphere will, in turn, depend on the temperature of the Earth's surface. Very high surface temperatures lead to the formation of a metal-oxide (e.g., Na, K, SiO, Mg) atmosphere [*Ringwood*, 1979]. Lower surface temperatures lead to the formation of a predominately H_2, CO, H_2O, CO_2, CH_4 atmosphere [*Holloway*, 1988], and still lower temperatures favor an air, e.g., N_2-rich, atmosphere. Liquid water would not be stable at the Earth's surface if the bulk of the mantle were molten or partially molten. Since such a molten state is the premise of our discussion, we will not consider the latter case.

The potential surface temperature of a totally molten Earth could exceed 3500 K (Figure 8*a*) if the entire mantle were completely molten. Under such conditions, a metal-oxide vapor atmosphere would form. However, condensation (i.e., the formation of oxide and silicate clouds) would probably limit the effective radiating temperature of the atmosphere to be ≈2000 K [*Thompson and Stevenson*, 1988]. The radiative blackbody heat flux corresponding to a temperature of 2000 K is $\sigma T^4 = 0.9$ MW/m^2, where σ is the Stefan-Boltzmann constant.

A H_2O, CO, or CO_2 atmosphere that would form at surface temperatures below ≈1500 K could similarly regulate the radiating temperature. The numerical experiments of *Zahnle et al.* [1988] indicate that for surface temperatures below about 1500 K, a water-rich atmosphere would limit the net radiative heat flux to about 150 W/m^2: about 6000 times less than a metal-

oxide atmosphere. For surface temperatures above 1500 K, the water-rich atmosphere is transparent to much of the surface radiation, which has significant components in visible and UV wavelengths. Consequently, the radiative properties of the atmosphere in the surface temperature interval of 1500-2000 K would be intermediate between the water-rich and metal-oxide cases.

As a first approximation, we adopt a mean heat flux of 0.9 MW/m^2 when the surface temperature exceeds 2000 K and a mean heat flux of 150 W/m^2 when the surface temperature drops below 1500 K. If there is no crust on the magma ocean, then the surface temperature will exceed 2000 K when the lower mantle of the Earth is crystallizing (Figure 8*a*), and the heat flux regulating fractionation of the lower mantle will be that corresponding to a metal-oxide atmosphere: 0.9 MW/m^2. If no crust exists when the upper mantle crystallizes, then the surface temperature will be between 1500 and 2500 K (Figure 8*b*), and the heat flow will be between 150 W/m^2 and 0.9 MW/m^2. If a crust forms, then the mean surface temperature cannot be greater than the solidus temperature of the crust, ≈1500 K, corresponding to a maximum heat flux of about 150 W/m^2, independent of the temperature of the underlying magma.

The impact of heat flux on chemical fractionation can be appreciated by considering the energy budget of the molten mantle. From Figure 8*a*, it can be seen that to generate a crystalline mantle about 1.7×10^{31} J (the sum of the energy differences between adiabatic profiles) must be removed from a wholly molten mantle beginning to crystallize at its base. The surface area of the Earth is about 5×10^{14} m^2. If the Earth cooled at a mean surface temperature greater than 2000 K, i.e., regulated by a metal-oxide atmosphere, then the cooling time would be only 1200 years! This case is tantamount to quenching the mantle, and chemical fractionation would be limited. If the mean heat flux were 150 W/m^2, i.e., regulated by a cooler water-rich atmosphere, then the cooling time would be 7.2×10^6 years. This longer time affords a greater opportunity for chemical fractionation to occur.

A crust on a superheated liquid mantle? The existence of a crust would be important for the chemical fractionation of the mantle because it would limit the maximum heat flux from the magma ocean to about 150 W/m^2, as discussed in the previous section, and possibly much less since heat transfer might be limited by conduction through the crust. An essential feature of a crust on a magma ocean is that it is not likely to be buoyant. *Morse* [1987] discussed this problem as it relates to a lunar magma ocean. Another feature of the early evolution of the magma ocean is that the ocean would necessarily be superheated at low pressure (Figure 8). A crust would thus have to support a very steep thermal gradient (at least $(T_{liquidus}-T_{solidus})/\delta$, where δ is the thickness of the crust), and foundered crust would dissolve unless it were thick [*Walker and Kiefer*, 1985]. Nevertheless, although a crust is not mechanically stable, is seems likely that some glass or crystals would form simply because convective heat transport may not keep pace locally with the extraordinarily high rate of radiative heat transport. In this subsection we investigate the importance of a crust when the upper mantle is superheated liquid.

Assuming that some crust can be generated but that it will ultimately sink because of its high density, we consider the possibility of a dynamically maintained crust. As a crude model, we consider a hypothetical pseudo-steady state crust of thickness δ. When it founders, blocks of diameter δ will sink according to Stokes' formula. Let us suppose that most of the radiative heat loss is applied to removing the latent heat of fusion of liquid that regenerates the crust. A crude heat balance is then given by

$$\frac{\delta^2\Delta\rho g}{18\eta}\rho\Delta H_f < F \approx \frac{\kappa(T_{liquidus}-T_{surface})}{\delta} \quad (9)$$

in units of energy per time per surface area. Here the radiative heat flux from the surface of the crust (second term) is balanced with conductive transport through the crust (third term). The heat flux necessary to regenerate foundered and melted crust (first term) must be less than this amount. Here, F is the heat flux from the magma ocean, η is the viscosity of the molten mantle (1 P), $\Delta\rho$ is the density contrast (200 kg/m^3) between the crust of density ρ (3000 kg/m^3) and the density of the liquid, ΔH_f is the latent heat of fusion (4×10^5 J/kg), and κ is the thermal conductivity (2 J/m K). The surface temperature, $T_{surface}$, must be below the 1-bar liquidus (2000 K) for crystals to form. In the initial stages of the evolution of the magma ocean, i.e., when the lower mantle is crystallizing, we assume that the temperature at the bottom of the crust will be approximately equal to the liquidus temperature.

If the heat flux is 150 W/m^2, we find that the crust cannot be thicker than 40 μm. The maximum heat flux, 0.9 MW/m^2, gives a maximum crust thickness of 2.6 mm but a surface temperature of 830 K that is inconsistent with such a high heat flux. The internally consistent solutions to (9) give a crust of negligible thickness. From this exercise we conclude that a dynamically maintained crust is not important from the perspective of heat transfer when the shallow regions of the magma ocean are superheated and thus that the heat flow from the magma ocean would have been controlled entirely by the atmosphere. Only in later stages of its evolution, when the magma ocean may contain crystals at all depths, will the viscosity near the surface increase because of crystal content and lower magma temperatures. This viscosity enhancement could stabilize a dynamic crust, allowing it to become an impediment to heat transfer. Even if dynamically stable, however, *Tonks and Melosh* [1990] note that the crust will be subject to disruption by shear stresses if the underlying magma is vigorously convecting.

Crystal-Liquid Fractionation in the Depth Range of the Lower Mantle

If the whole Earth were molten, then the adiabats shown in Figure 8*a* indicate that crystallization would have begun at the core-mantle boundary. From Figure 7 we believe that the first phase to crystallize would be perovskite. Any crystal-liquid segregation that occurred during the crystallization of the lower mantle would have perturbed the chemistry of the upper mantle if the liquid portion of the magma ocean were well mixed. *Agee and Walker* [1988*b*, 1989] suggest on the basis of a major element mass balance that some perovskite fractionation is required to generate the modern peridotitic upper mantle. *Ringwood et al.* [1987], *Kato et al.* [1988*a*, *b*, 1989], and *Ringwood* [1990] argue, however, that perovskite fractionation could not have been important because of trace element partitioning constraints. We showed earlier that perovskite may be less dense than a chondritic melt at the conditions of the deepest lower mantle (M1, Figure 9*b*); thus perovskite might segregate in a quiescent mantle by flotation at P>70 GPa (d>1680 km) and by settling at P<70 GPa, possibly generating the chemical fractionations inferred by *Agee and Walker* [1988*b*, 1989]. In a large convecting magma body, however, the flow regime will ultimately govern the extent to which segregation is possible.

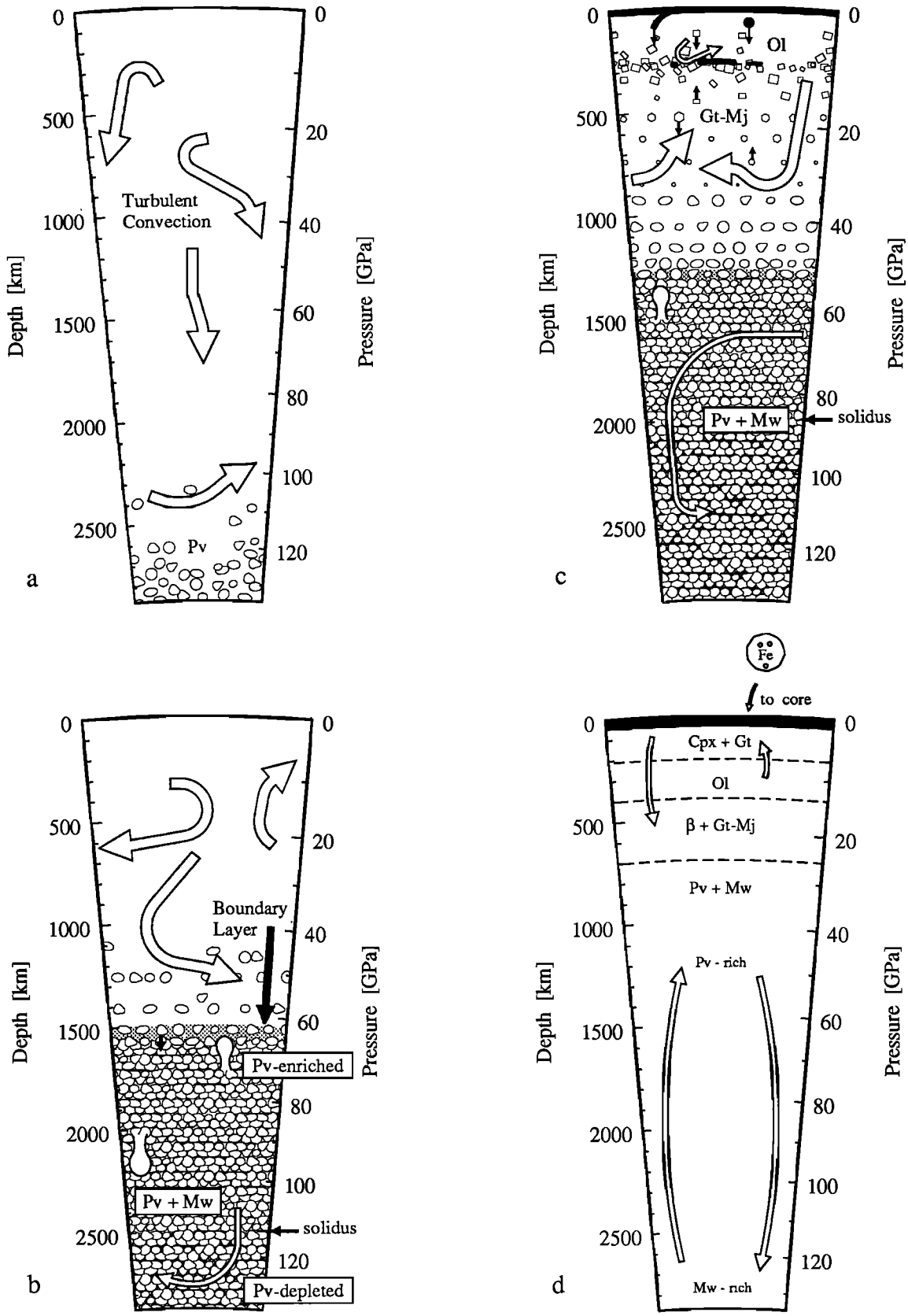

Fig. 9. Cartoon snapshots of the evolution of the mantle from an initial wholly molten state. (*a*) The first crystals to form will be perovskite at the base of the lower mantle. Crystal-liquid fractionation cannot occur although perovskite is likely to be buoyant. (*b*) In this snapshot, a boundary layer exists in the shallower lower mantle, and perovskite crystals may be capable of settling downward at this boundary. In this shallow region, perovskite-depleted liquid could percolate through the perovskite matrix to be mixed into the convecting liquid above. Below the the level of perovskite neutral buoyancy, percolating iron-rich perovskite-depleted liquid could sink. The deep crystalline lower mantle may begin subsolidus convection. (*c*) When the upper mantle begins to crystallize, a mechanically unstable crust may begin to form. Stagnant boundary layers on the unmelted foundered crust would allow olivine crystals to segregate from the magma leading to the formation of a dunite septum. Garnet-majorite cannot fractionate until the "floor" of the magma ocean reaches the garnet-majorite stability horizon. The crystalline deep lower mantle is undergoing subsolidus convection. (*d*) A schematic representation of the (gravitationally unstable) stratification of the mantle before subsolidus convection and possible rehomogenization takes place.

Perovskite settling/flotation in a convecting system. We assume the condition for segregation in a convecting fluid in the absence of boundary layers is that the settling velocity of the crystals exceeds the convective velocity of the magma. We can estimate the convective velocity of the magma ocean with mixing length theory [*Clayton*, 1968, pp. 252-259]:

$$v_{conv} \approx \left[\frac{d\,F}{H_T\,\rho}\right]^{1/3}, \tag{10}$$

where F is the surface heat flux, d is the depth of the ocean, and H_T is the thermal scale height:

$$H_T = \frac{T}{\rho g \left.\frac{\partial T}{\partial P}\right|_S}, \tag{11}$$

which we calculate to be approximately 2×10^4 km. Note that the convective velocity is weakly dependent on the heat flux. Recall that we have assumed the heat flux to be about 0.9 MW/m^2 during crystallization of the lower mantle. The average convective velocity for a 2900 km deep magma ocean is then about 3 m/s.

For crystal segregation to occur, the settling (or rising) velocity must exceed the vertical component of the convective velocity. In a low Reynolds number regime ($\mathrm{Re}\equiv 2rv\rho/\eta$ for $\mathrm{Re} \le 2$, where the Reynolds number, Re, is evaluated for crystals. Here r is the crystal radius, v is the relative crystal-liquid velocity approximated by (10), η is the fluid viscosity, g is the gravitational acceleration, ρ is the fluid density, and $\Delta\rho$ is the density contrast. This is not the Reynolds number characterizing the convective flow of the magma ocean) the settling velocity is well approximated by Stokes' terminal velocity formula. In higher Re regimes a variety of empirical relationships can be used to determine settling velocities [*Bird et al.*, 1960]:

$$\mathrm{Re} \le 2: \qquad r \approx \left[\frac{9\eta v}{2g\Delta\rho}\right]^{1/2} \tag{12a}$$

$$2 \le \mathrm{Re} \le 500: \qquad r \approx \left[\frac{111\rho v^2}{16g\Delta\rho}\right]^{5/8}\left[\frac{\eta}{2v\rho}\right]^{3/8} \tag{12b}$$

$$500 \le \mathrm{Re} \le 2\times10^5: \qquad r \approx \frac{33\rho v^2}{200g\Delta\rho} \tag{12c}$$

Note that the viscosity dependence of r is different in each flow regime, and (12*c*) is independent of viscosity. The dependence of crystal size on the assumed heat flux is also different in each regime. Comparing (10) with (12), we see that crystal size is proportional to $F^{1/6}$ (equation (12*a*)), $F^{7/24}$ (equation (12*b*)), or $F^{2/3}$ (equation (12*c*)). We estimate the crystal size by evaluating each of these equations, determining the Reynolds number for each case, and selecting the result that is consistent with the Re conditions. For perovskite in the lower mantle, the maximum crystal-liquid density contrast will be $\approx$0.25 g/cm^3. If the viscosity of molten C1 obeys an Arrhenius relationship, independent of pressure, then we would estimate a lower limit for the viscosity to be $\approx$ 0.01 P [*Bottinga and Weill*, 1972]. The combined pressure and temperature dependence of viscosity is unknown for silicate liquids under these conditions so this value for viscosity must be suspect. However, we estimate that crystals 60 m (!) in diameter would be required if segregation is to occur in such a vigorously convecting system, independent of viscosity (Re is 8×10^8 in this case, outside the bounds of the constitutive relations). If we considered a heat flux 10^3 times smaller, then the velocity would be 30 cm/s, and the required crystal diameter would be 60 cm. While EOS constraints alone might suggest crystal flotation or settling during lower mantle crystallization, consideration of the flow characteristics in a magma ocean emphatically precludes this possibility.

Boundary layer processes. As a magma ocean cools, a crystal-rich layer will develop at its base (Figure 9). This crystal enrichment is not a consequence of crystal settling but is simply a result of the wet adiabat approaching the solidus. This crystal enrichment leads to rapidly increasing viscosity, which in turn could lead to a change in the flow structure of the ocean. According to *Roscoe*'s [1953] criterion, 44% (by volume) of crystals would increase the viscosity over the crystal-free viscosity by a factor of 10, about the maximum viscosity contrast the system can tolerate before forming a boundary layer [*Marsh*, 1989].

If a boundary layer forms in the lower mantle between crystal-poor magma above and crystal-rich magma below, then chemical fractionation could occur through two mechanisms. First, crystal settling or flotation could occur through this boundary layer, regardless of crystal size, since the moving crystals would not have to oppose convective flow. Second, interstitial liquid could be expelled from the compacting crystal-rich zone beneath the boundary layer by matrix compaction. If crystals are denser than liquid, then interstitial liquid will be expelled upward, leading to chemical fractionation effects in the upper mantle by upward transport of perovskite-depleted liquid. If crystals are less dense than the liquid, then expelled liquid will segregate downward and the boundary zone will be enriched in crystals. Any melt segregated downward would be hidden from the upper mantle, which would thus be unaffected by this fractionation. However, if the buoyant crystals in the boundary layer become entrained and redissolved in the convecting liquid above the boundary layer, then chemical fractionation could also occur in the overlying magma.

In the lower mantle, our results suggest perovskite would be buoyant in C1-like liquid compositions at pressures $\ge$70 GPa (1680 km) and more dense than the liquid at lower pressures (M1, Figure 9*b*). As the lower mantle crystallizes, the nature of possible chemical fractionation at the boundary layer would therefore change. When the boundary layer is at greater pressure than the perovskite neutral buoyancy horizon ($\approx$70 GPa), perovskite will tend to float. If boundary layer entrainment can occur, dissolution of the entrained crystals would enrich in perovskite components the still largely molten and superheated, convecting portion of the magma ocean above the boundary layer. At later times, when the boundary layer is shallower than the perovskite neutral buoyancy horizon, perovskite will tend to settle out from the boundary layer, possibly promoting the formation of perovskite-enriched cumulates and depletion of the overlying magma in perovskite components. The combined effect, early enrichment of the ocean in buoyant, entrained perovskite followed by deposition of perovskite from the perovskite-enriched magma, would be a net enrichment of the <70 GPa region of the crystallizing lower mantle in perovskite components relative to the deeper lower mantle. Later, under subsolidus conditions, this chemical stratification would be unstable because crystalline perovskite is denser than crystalline magnesiowüstite. The formation of such a stratified lower mantle might therefore promote subsequent subsolidus convection.

Matrix compaction in the zone beneath the boundary layer could also result in an overall depletion of the deepest mantle in

perovskite components. Iron-rich interstitial liquids in the crystal-rich regions below the boundary layer would tend to sink, thereby enriching in perovskite components that part of the lower mantle from which the interstitial liquid drains. The deeper lower mantle in which this interstitial liquid collects would become correspondingly depleted in perovskite components through enrichment in magnesiowüstite components. At pressure ≤70 GPa, differentiated interstitial liquid might rise to mix with the overlying magma. The combined effect would be to enrich in perovskite components that part of the lower mantle near the perovskite neutral buoyancy horizon and perhaps to progressively deplete the still liquid parts of the magma ocean in perovskite as the ocean continues to crystallize.

The two fractionation mechanisms discussed above could create a perovskite component gradient in the lower mantle, especially in the vicinity of the perovskite neutral buoyancy horizon. These mechanisms do not, however, necessarily imply that the upper mantle would be depleted in perovskite components relative to the bulk mantle. The magma from which the upper mantle would ultimately have crystallized might have become initially enriched in perovskite components when the boundary layer was deeper than 70 GPa but would later have become depleted in these same components as crystallization continued in the 25-70 GPa interval. The relative efficiency of these fractionation mechanisms, and thus whether the upper mantle would become enriched or depleted overall in perovskite components, is difficult to assess. The mechanism that depletes the magma in perovskite components acts on a larger volume of mantle than the mechanism that enriches the magma in perovskite components (i.e., the volume of the 25-70 GPa region is about 34% greater than that of the 70-136 GPa region). Also, convective velocities are expected to slow as time progresses, favoring more efficient fractionation at later times. These factors might favor the possibility of overall depletion of the upper mantle in perovskite components.

The extent of perovskite fractionation by settling crystals through a boundary layer is difficult to quantify since the crystal content and velocities of turbulent eddies near the boundary layer must be known. Crystal size, which must also be known, depends on the mean residence time of eddies in the subliquidus region of the magma ocean and the kinetics of crystal growth. A simple model for crystal settling in a turbulently convecting magma body was developed by *Martin and Nokes* [1988]. Their model is based on experimental measurements in the limit of very low crystallinity (≈0.3 vol %). Since the crystal fraction near the boundary layer could be very large, ≈44 vol %, their model is not directly applicable in this case. When the crystal fraction in the boundary layer is large, the viscosity and hence settling rate for individual crystals is strongly dependent on the crystal content. In this limit, the problem of crystal settling through a boundary layer becomes in essence a problem of matrix compaction. Perovskite fractionation by matrix compaction is more easily quantified and gives a lower limit to the amount of perovskite fractionation that could occur. This mechanism is discussed below.

Perovskite fractionation by matrix compaction. To what extent could matrix compaction lead to fractionation in a magma ocean? We are interested in the case where liquid is expelled from a compacting matrix that is undergoing crystallization and that is growing in vertical extent because of the crystallization of the overlying liquid. This compacting region may also be convecting. To evaluate this mechanism, we will first estimate the characteristic velocity of the compacting matrix with the method of *Richter and McKenzie* [1984] and *McKenzie* [1984]; then we will compare this velocity to the upward velocity of the solidus in the cooling lower mantle. The characteristic velocity of the compacting matrix is given by [*Richter and McKenzie*, 1984]

$$v_c = \frac{k_0}{\eta}(1-\phi_0)\Delta\rho g \ , \qquad (13)$$

where k_0 is the permeability, $\Delta\rho$ is the density contrast, and ϕ_0 is the initial volume fraction of the fluid phase. Let us consider the case $\phi_0 = 0.56$, obtained above from Roscoe's criterion for a 10× viscosity increase. Conservative estimates of the remaining terms are $\eta = 1$ P, $k_0 = 1.7\times10^{-4}$ cm^2 (using the constitutive relationship given by (5) of *Richter and McKenzie* [1984], and assuming a crystal radius of 1 cm), and $\Delta\rho = 0.2$. With these assumptions, the characteristic matrix velocity is 0.5 km/yr, proportional to the crystal size squared.

The time scale for the growth of the crystal-rich layer can be estimated from the heat flux from the magma body. Given the heat flux (0.9 MW/m^2), we calculate the growth of the layer from the difference in heat and crystal content of the adiabatic profiles (Figure 8) to be about 2.6 km/yr. Since the liquidus and solidus of the lower mantle are subparallel, the velocity of the solidus will also be ≈2.6 km/yr. Although the velocity of the solidus exceeds the velocity of the compacting matrix by a factor of 5, we consider them to be roughly comparable (since neither the heat flux, viscosity, nor crystal size are well-constrained parameters), and thus that matrix compaction could, under some circumstances, lead to significant chemical fractionation effects in the lower mantle. In any case, matrix compaction or initial inhomogeneities in initial crystal fractions in the partially molten zones could generate regions of locally high fluid fraction that could ascend rapidly either as diapirs or solitary waves [*Richter and McKenzie*, 1984; *Scott and Stevenson*, 1984, 1986, 1988]. Some fractionation by auxiliary diapiric processes or enchanced porous flow as magmons may be possible even if the compaction rate is much smaller than the crystallization rate. We thus conclude that perovskite fractionation by matrix compaction could have been a significant fractionation process in a global magma ocean, but the extent to which it would occur depends strongly on poorly constrained model parameters.

Crystal-Liquid Fractionation in the Depth Range of the Upper Mantle and Transition Zone

Garnet-majorite crystallization. When garnet-majorite begins to crystallize, perovskite crystallization is still incomplete in the lower mantle (Figure 8), and the floor (>44% crystals) of the magma ocean is deeper (≈40 GPa; ≈1000 km) than the garnet-majorite→perovskite reaction boundary. Thus, if the initially crystallized garnet-majorite were able to sink, it would convert to perovskite before reaching the floor of the magma ocean. Only when the floor of the magma ocean reaches the garnet-majorite → perovskite reaction boundary at 25 GPa would fractionation of garnet-majorite components be possible by such a mechanism. We note, however, that garnet-majorite is predicted to be neutrally buoyant in komatiitic liquid at ≈22 GPa (M1, Figure 8). Thus, when garnet-majorite first crystallizes in the magma ocean, it may resist fractionation because of its neutral buoyancy, although it might even have a tendency to float and thus to be digested by and enriched in the overlying superheated liquid. We consider this to be unlikely given the difficulty of

crystal-liquid segregation in such a system except in the vicinity of boundary layers. However, once olivine begins to crystallize in the upper mantle, a boundary layer or "septum" could develop in the upper parts of the magma ocean that might isolate the shallow upper mantle from the effects of garnet-majorite fractionation [*Agee and Walker*, 1988*b*].

Olivine crystallization and the formation of a dunite septum. The prediction that olivine would be less dense than ultrabasic liquid near 8 GPa led *Nisbet and Walker* [1982], *Ohtani* [1985], and *Agee and Walker* [1988*b*] to suggest that a dunite septum would develop at the depth of olivine neutral buoyancy. Such a septum would separate the magma ocean into upper and lower regions that could evolve separately. The lower magma reservoir has been suggested by these authors as a source of komatiitic magma. In this subsection we will address the feasibility of this proposition.

The phase diagram (Figure 8*b*) suggests that olivine will first begin to crystallize near its neutral buoyancy horizon (although it is not clear how relevant this phase diagram would be if perovskite fractionation in the earlier history of the magma ocean had been efficient). Olivine fractionation could therefore probably not have been efficient initially since at neutral buoyancy there is no gravitational driving force for fractionation. However, as the mantle continued to cool, olivine would crystallize both above and below the neutral buoyancy horizon. When olivine first begins to crystallize, the transition zone will be nearly 10% crystalline, and the 25-70 GPa interval of the lower mantle will be nearly 60% crystalline. As the upper mantle cools beyond this point, regions both above and below the olivine neutral buoyancy point will begin to crystallize olivine. If a dunite septum develops and grows, it would do so by both olivine settling from above and flotation from below, so the magma reservoirs above and below the septum could both be depleted in olivine (and possibly perovskite, as discussed above). Would such crystals segregate from liquid, for example, at the surface of the magma ocean, where the density contrast between crystal and liquid is maximized? The convective velocity (from the mixing length formula (equation (10)) with a heat flux of 150 W/m^2) of the magma ocean will be approximately 10 cm/s. We estimate that the viscosity of crystal-free magma will be ≈1 P [*Bottinga and Weill*, 1972]. With these assumptions, a crystal radius of ≥3.5 cm (equation (12*b*)) is required for crystal flotation/settling to occur in the absence of a boundary layer. As discussed previously, this result is weakly dependent on the assumed heat flux (r is proportional to $F^{7/24}$ in this flow regime). Olivine segregation by settling or flotation could occur if ≈3.5 cm crystals could form; this crystal size is proportional to the 3/8 power of viscosity, which could readily be an order of magnitude higher or lower. Crystals of this size do not, a priori, seem unreasonable, but whether they could form depends on the kinetics of crystals growth and on the mean residence time of turbulent eddies in the shallow mantle where olivine is the liquidus phase.

Agee and Walker [1988*b*] proposed an alternative mechanism for nucleating a septum that circumvents the need for large single crystals. They proposed that meter-sized foundered blocks of crust would sink without dissolving [*Walker and Kiefer*, 1985] and come to rest near the level of olivine neutral buoyancy. Olivine crystals in the magma could then accumulate above and below the foundered crust through stagnant boundary layers or compaction processes (Figure 9*c*). In this case, the formation of a dunite cumulate layer depends critically on the details of crust formation and crust stability. That the young crust would have been dense and subject to disruption by the turbulent motion of the magma ocean [*Tonks and Melosh*, 1990], as discussed above, is consistent with *Agee and Walker*'s [1988*b*] mechanism. Once nucleated, a septum could grow by boundary layer processes such as those discussed above in connection with perovskite fractionation in the lower mantle even in the presence of vigorous convection.

If an olivine septum developed, where would it be situated as the system evolved? Olivine below the neutral density horizon is buoyed up by a force proportional to the density contrast. Olivine above the neutral buoyancy horizon will experience a similar force, but of opposite sign, that pushes the septum downward. The septum will situate itself in a position where these forces are exactly balanced (Archimedes' principle). If crystal accumulation from below were not properly balanced by crystal accumulation from above, then the positive and negative buoyancy forces would not balance. The septum would have to readjust, and this readjustment would necessitate magma transport through the septum. The "septum" would therefore be permeable. Transport of magma through the permeable septum could transmit chemical fractionations between the upper and lower magma reservoirs, in a direction dependent on the relative crystallization rates of the two reservoirs. It seems likely that the upper, shallow reservoir would crystallize faster. If this were so, then downward settling of the dunite septum would force magma from the lower reservoir through the permeable septum to mix with the upper magma reservoir. When the floor of the magma ocean (≈ 44% crystallinity) reaches the level of garnet-majorite stability (relative to perovskite), the magma trapped between this floor and the dunite cumulate layer could become depleted in garnet-majorite. To the extent that this garnet-majorite-depleted magma could traverse the dunite cumulate layer (as this layer sagged downward due to addition of olivine from above faster than from below) and mix with the overlying magma, regions above the dunite septum might develop a garnet-majorite-depleted chemical signature. A garnet-majorite fractionation signature in the shallow upper mantle might thus be subdued by the development of a dunite cumulate layer, but cannot be entirely excluded.

Post-Crystallization Rehomogenization Processes

The evolution of the Hadean mantle from an initially molten state described above would likely lead to some chemical heterogeneity in the upper mantle [cf. *Melosh and Tonks*, 1989; *Tonks and Melosh*, 1990]. For example, perovskite, garnet-majorite, and/or olivine fractionation could have occurred, and, indeed, aspects of the chemistry of mantle rocks and seismic properties of the mantle have been used to infer that they did. However, even if such fractionations occurred, their most extreme manifestations may have been obliterated by subsequent rehomogenization of the mantle by subsolidus convection after most of the mantle crystallized. For example, *Ohtani* [1985] and *Agee and Walker* [1988*b*] noted that the shallow upper mantle, depleted in olivine components by the formation of the dunite cumulate layer, would crystallize to a denser clinopyroxene and garnet assemblage. Convective overturn might later place the olivine-enriched cumulate at the base of the crust or remix these fractionated components. The extent to which such overturn and rehomogenization could have occurred would depend on the vertical extent of the mantle convection system, and whether the mantle convected in one, two, or many layers. This in turn depends on the extent to which chemical

stratification developed during crystallization. However, that the upper and lower mantle and perhaps the transition zone may differ in composition today [e.g., *Jeanloz and Knittle*, 1989; *Anderson*, 1989] may suggest that convective rehomogenization was limited to specific regimes within the mantle.

Tonks and Melosh [1990] recently independently considered the possibility of chemical fractionation in a global magma ocean. While the details of their model are somewhat different than ours, their basic conclusions are compatible with ours. (1) They argue, as do we, that turbulent convection in a global magma ocean will suspend crystals until the system becomes choked by high crystal content. (2) Where the crystal content is large, the system will form two separate layers. They do not consider the possible impact of the implicit boundary layer on fractionation. (3) Percolation of liquid within the zone of high crystallinity will not advance as rapidly as the boundary layer. These conclusions accord with ours that dynamical processes tend to limit the extent of chemical fractionation that would be possible in a global magma ocean. However, *Tonks and Melosh*'s [1990, p. 151] statement that "a totally molten initial Earth may have failed to differentiate by fractional crystallization" overstates, in our view, the impact of these dynamical processes since they diminish in importance in the later stages of crystallization (e.g., when a dunite "septum" might form) and at all boundary layers. Based on our analysis, these late stage differentiation processes and processes occurring at boundary layers could lead to significant chemical fractionations.

4. CONCLUSIONS

We have applied our komatiite EOS data to the problem of adiabatic melting. We constructed a model that allows us to compute the melt fraction of adiabatic diapirs in a peridotitic mantle. Because the liquidus and solidus are subparallel to the adiabats, the melt fraction of diapirs remains essentially constant in the 250-450 km range of the upper mantle. Komatiitic liquids in equilibrium with olivine ± clinopyroxene ± garnet can be formed by 30% partial melting of fertile peridotite at 5.6 GPa. The model is also compatible with the view that komatiites represent >30% melting if they are in equilibrium with olivine only and if they separate from their residue at lower pressures. Both views require that an initially solid mantle diapiric source of komatiites begin melting at depths in excess of 500 km (i.e., in the transition zone or lower mantle). Our model for the petrogenesis of komatiitic liquids by adiabatic melting is much like that for the petrogenesis of picrites or MORB but requires significantly hotter (>700°) diapirs that begin melting at greater depths within the mantle.

We have discussed the early stages of the evolution of a magma ocean. The formation and evolution of a molten mantle are highly dependent on the accretion scenario and cannot be modeled on the basis of EOS and phase equilibrium constraints alone. Issues that are difficult to address include (1) the time scale of Earth accretion, (2) the rheological and physical processes that occur in turbulent convection in a deep system without walls, (3) rates of heat transfer through different protoatmospheres that form in response to different rates of planetesimal accretion, (4) the dynamics of crust formation and recycling on a magma ocean, and (5) the dynamics of subsolidus convection to the extent this governs rehomogenization of the Earth. Future work should address the specific flow structure of the magma ocean, and the specific nature of the coexisting atmosphere.

Despite the simplicity of our calculations, several conclusions can be drawn: (1) If the mantle were adiabatic, the wholly molten mantle would crystallize from the bottom up. When crystallization begins in the upper mantle, most of the transition zone and lower mantle would still be partially molten. (2) A crust at the surface of the magma ocean would not have been stable while the crystallization front traversed the lower mantle. The surface temperature of the magma ocean would have been between 1900° and 3200°C, favoring the existence of a metal-oxide atmosphere. (3) Although perovskite would tend to float at depths of ≥1680 km and sink at shallower depths, convective velocities in a magma ocean this deep would be so high as to prevent crystal-liquid segregation. However, as the system cools, the degree of crystallinity at depth along an adiabat becomes high enough (≥44%) that the less crystalline part of the system above this level and the more crystalline part below begin to convect separately. Crystal settling/flotation could occur at the boundary between these layers. Matrix compaction in the lower level could lead to expulsion of liquid downward at depths >1680 km and upward at depths <1680 km. Diapirism could facilitate this fractionation process. This could lead to effective fractionation of perovskite components in the liquid of the upper mantle. (4) When garnet-majorite first begins to crystallize, the floor of the magma ocean would be deeper than the maximum depth of garnet-majorite stability. Garnet-majorite would therefore be initially inhibited from fractionating because it would not be stable in the boundary layers or deeper cumulate pile in which crystal-liquid fractionation would be most favored. In any case, garnet-majorite is expected to be nearly neutrally buoyant under these conditions, so fractionation would be minimal even if it could be brought into a boundary layer. Garnet-majorite fractionation may become possible when the floor of the magma ocean rises to sufficiently shallow levels; at this stage in the magma ocean evolution, the formation of a dunite septum might limit, but would probably not completely exclude, garnet-majorite fractionation effects in the upper mantle. (5) A dunite cumulate layer might form in the upper mantle, either by the settling and/or rising of individual crystals or by the accumulation of crystals around foundered crust. Such a septum, although it would probably inhibit communication between the regions of magma above and below it and separate them into distinct convecting regimes, would necessarily be permeable; thus, although it could limit the extent of a signature of garnet-majorite fractionation effects in the region above it, it would not eliminate it altogether.

Acknowledgements. We are grateful to D.J. Stevenson, D.L. Anderson, and N.T. Arndt (Max-Planck-Institut für Chemie, Mainz) for their thoughtful comments and suggestions. We also thank K. Wei and R.G. Tronnes (University of Alberta) for sharing his unpublished manuscript with us. This manuscript has benefited greatly from the thoughtful review of D. Walker. This work was funded by the National Science Foundation grants EAR-86-18545 and EAR-89-16753. Contribution 4809, Division of Geological and Planetary Sciences, California Institute of Technology, Pasadena, California.

REFERENCES

Abe, Y., and T. Matsui, Early evolution of the Earth: Accretion, atmosphere formation, and thermal history, *Proc. Lunar Planet. Sci. Conf. 17th*, part 1, *J. Geophys. Res., 91*, suppl., E291-E302, 1986.

Agee, C.B., A new look at differentiation of the Earth from melting experiments on the Allende meteorite, *Nature, 346*, 834-837, 1990.

Agee, C.B., and D. Walker, Static compression and olivine flotation in ultrabasic silicate liquid, *J. Geophys. Res., 93*, 3437-3449, 1988*a*.

Agee, C.B., and D. Walker, Mass balance and phase density constraints on early differentiation of chondritic mantle, *Earth Planet. Sci. Lett., 90*, 144-156, 1988*b*.

Agee, C.B., and D. Walker, Comments on "Constraints on element partition coefficients between $MgSiO_3$ perovskite and liquid determined by direct measurements" by T. Kato, A.E. Ringwood and T. Irifune, *Earth Planet. Sci. Lett., 94*, 160-161, 1989.

Ahrens, T.J., Earth accretion, in *Origin of the Earth*, edited by H.E. Newsom and J.H. Jones, pp. 211-227, Oxford University Press, New York, 1990.

Anderson, D.L., Chemical inhomogeneity of mantle above 670 km transition, *Nature, 307*, 114, 1984.

Anderson, D.L., Composition of the Earth, *Science, 243*, 367-370, 1989.

Arndt, N.T., Ultrabasic magmas and high-degree melting of the mantle, *Contrib. Mineral. Petrol., 64*, 205-221, 1977.

Benz, W., W.L. Slattery, and A.G.W. Cameron, The origin of the Moon and the single-impact hypothesis I, *Icarus, 66*, 515-535, 1986.

Benz, W., W.L. Slattery, and A.G.W. Cameron, The origin of the Moon and the single-impact hypothesis, II, *Icarus, 71*, 30-45, 1987.

Bickle, M.J., C.E. Ford, and E.G. Nisbet, The petrogenesis of peridotitic komatiites: Evidence from high-pressure melting experiments, *Earth Planet. Sci. Lett., 37*, 97-106, 1977.

Birch, F., Energetics of core formation, *J. Geophys. Res., 70*, 6217-6221, 1965.

Bird, R.B., W.E. Stewart, and E.N. Lightfoot, *Transport Phenomena*, pp. 190-196, John Wiley, New York, 1960.

Bottinga, Y., and D.F. Weill, The viscosity of magmatic silicate liquids: A model for calculation, *Am. J. Sci., 272*, 438-475, 1972.

Cameron, A.G.W, and W. Benz, Possible scenarios resulting from the giant impact (abstract), *Lunar Planet. Sci. Conf., 20*, 137-138, 1989.

Campbell, I.H., R.W. Griffiths, and R.I. Hill, Melting in an Archaean mantle plume: Heads it's basalts, tails it's komatiites, *Nature, 339*, 697-699, 1989.

Carmichael, I.S.E, F.J. Turner, and J. Verhoogen, *Igneous Petrology*, 739 pp., McGraw-Hill, New York, 1974.

Cawthorn, R.G., Degrees of melting in mantle diäpirs and the origin of ultrabasic liquids, *Earth Planet. Sci. Lett., 27*, 113-120, 1975.

Clayton, D.D., *Principles of Stellar Evolution and Nucleosynthesis*, 612 pp., McGraw-Hill, New York, 1968.

DeWit, M.J., R.A. Hart, and R.J. Hart, The Jamestown Ophiolite Complex, Barberton mountain belt: A section through 3.5 Ga oceanic crust, *J. Afr. Earth Sci., 6*, 681-730, 1987.

Echeverria, L.M., Komatiites from Gorgona Island, Colombia, in *Komatiites*, edited by N.T. Arndt and E.G. Nisbet, pp. 199-209, George Allen and Unwin, Boston, Mass., 1982.

Elthon, D., and C.M. Scarfe, High-pressure phase equilibria of a high-magnesia basalt and the genesis of primary oceanic basalts, *Am. Mineral., 69*, 1-15, 1984.

Gansser, A., V.J. Dietrich, and W.E. Cameron, Paleogene komatiites from Gorgona Island, *Nature, 278*, 545-546, 1979.

Green, D.H., Genesis of Archean peridotitic magmas and constraints on Archean geothermal gradients and tectonics, *Geology, 3*, 15-18, 1975.

Green, D.H., W.O. Hibberson, and A.L. Jaques, Petrogenesis of mid-ocean basalts, in *The Earth: Its Origin, Structure, and Evolution*, edited by M.W. McElhinney, pp. 265-299, Academic, San Diego, Calif., 1979.

Heinz, D.L., and R. Jeanloz, Measurement of the melting curve of $Mg_{0.9}Fe_{0.1}SiO_3$ perovskite at lower mantle conditions and its geophysical implications, *J. Geophys. Res., 92*, 11,437-11,444, 1987.

Herzberg, C.T., Solidus and liquidus temperatures and mineralogies for anhydrous garnet-lherzolite to 15 GPa, *Phys. Earth Planet. Inter., 32*, 193-202, 1983.

Herzberg, C.T., and M.J. O'Hara, Origin of mantle peridotite and komatiite by partial melting, *Geophys. Res. Lett., 12*, 541-544, 1985.

Herzberg, C.T., M. Feigenson, C. Skuba, and E. Ohtani, Majorite fractionation recorded in the geochemistry of peridotites from South Africa, *Nature, 332*, 823-826, 1988.

Hess, P.C., Komatiites and the Archean mantle (abstract), *Proc. Lunar Planet. Sci. Conf., 21*, 501-502, 1990.

Holloway, J.R., Planetary atmospheres during accretion: The effect of C-O-H-S equilibria, abstract, *Lunar Planet. Sci. Conf, 19*, 449-500, 1988.

Houghton, J.T., *The Physics of Atmospheres*, Cambridge University Press, New York, 1977.

Ito, E., and E. Takahashi, Melting of peridotite at uppermost lower-mantle conditions, *Nature, 328*, 514-517, 1987.

Jahn, B.M., G. Gruau, and A.Y. Glikson, Komatiite of the Onverwacht Group, S. Africa: REE geochemistry, Sm/Nd age and mantle evolution, *Contrib. Mineral. Petrol., 80*, 25-40, 1982.

Jarvis, G.T., and I.H. Campbell, Archean komatiites and geotherms: Solution to an apparent contradiction, *Geophys. Res. Lett., 10*, 1133-1136, 1983.

Jeanloz, R., Thermodynamics of phase transitions, *Rev. Mineral., 14*, 389-429, 1985.

Jeanloz, R., and E. Knittle, Density and composition of the lower mantle, *Philos. Trans. R. Soc. London, Ser. A, 328*, 377-389, 1989.

Jeanloz, R., and F.M. Richter, Convection, composition, and the thermal state of the lower mantle, *J. Geophys. Res., 84*, 5497-5504, 1979.

Kato, T., A.E. Ringwood, and T. Irifune, Experimental determination of element partitioning between silicate perovskites, garnets and liquids: Constraints on early differentiation of the mantle, *Earth Planet. Sci. Lett., 89*, 123-145, 1988*a*.

Kato, T., A.E. Ringwood, and T. Irifune, Constraints on element partition coefficients between $MgSiO_3$ perovskite and liquid determined by direct measurements, *Earth Planet. Sci. Lett., 90*, 65-68, 1988*b*.

Kato, T., A.E. Ringwood, and T. Irifune, Constraints on element partition coefficients between $MgSiO_3$ perovskite and liquid determined by direct experimental measurements - Reply to C.B. Agee and D. Walker, *Earth Planet. Sci. Lett., 94*, 162-164, 1989.

Kaula, W.M., Thermal evolution of Earth and Moon growing by planetesimal impacts, *J. Geophys. Res., 84*, 999-1008, 1979.

Knittle, E., and R. Jeanloz, Melting curve of $(Mg,Fe)SiO_3$ perovskite to 96 GPa: Evidence for a structural transition in lower mantle melts, *Geophys. Res. Lett., 16*, 421-424, 1989.

Lees, A.C., M.S.T. Bukowinski, and R. Jeanloz, Reflection properties of phase transition and compositional change models of the 670-km discontinuity, *J. Geophys. Res., 88*, 8145-8159, 1983.

Marsh, B.D., On convective style and vigor in sheet-like magma chambers, *J. Petrol., 30*, 479-530, 1989.

Martin, D., and R. Nokes, Crystal settling in a vigorously convecting magma chamber, *Nature, 332*, 534-536, 1988.

Matsui, T., and Y. Abe, Formation of a "magma ocean" on the terrestrial planets due to the blanketing effect of an impact-induced atmosphere, *Earth Moon Planets, 34*, 223-230, 1986.

McKenzie, D., The generation and compaction of partially molten rock, *J. Petrol., 25*, 713-765, 1984.

McKenzie, D., and M.J. Bickle, The volume and composition of melt generated by extension of the lithosphere, *J. Petrol., 29*, 625-679, 1988.

Melosh, H.J., and W.B. Tonks, Giant impacts, global magma oceans and geochemical differentiation: A view of the Earth's early thermal regime (abstract), *Eos Trans. AGU, 70*, 1000, 1989.

Mercier, J.-C., and N.L. Carter, Pyroxene geotherms, *J. Geophys. Res., 80*, 3349-3362, 1975.

Miller, G.H., E.M. Stolper, and T.J. Ahrens, The equation of state of a molten komatiite, 1, Shock wave compression to 36 GPa, *J. Geophys. Res.*, this issue.

Morse, S.A., Origin of earliest planetary crust: Role of compositional convection, *Earth Planet. Sci. Lett., 81*, 118-126, 1987.

Nesbitt, R.W., S. Sun, and A.C. Purvis, Komatiites: Geochemistry and genesis, *Can. Mineral., 17*, 165-186, 1979.

Nisbet, E.G., and D. Walker, Komatiites and the structure of the Archaean mantle, *Earth Planet. Sci. Lett., 60*, 105-113, 1982.

O'Hara, M.J., M.J. Saunders, and E.P.L. Mercy, Garnet-peridotite, primary basaltic magma and eclogites; Interpretation of upper mantle processes in kimberlite, *Phys. Chem. Earth, 9*, 571-604, 1975.

Ohtani, E., Melting temperature distribution and fractionation in the lower mantle, *Phys. Earth Planet. Inter., 33*, 12-25, 1983.

Ohtani, E., The primordial terrestrial magma ocean and its implications for stratification of the mantle, *Phys. Earth Planet. Inter., 38*, 70-80, 1985.

Ohtani, E., Generation of komatiite magma and gravitational differentiation in the deep upper mantle, *Earth Planet. Sci. Lett., 67*, 261-272, 1984.

Ohtani, E., and H. Sawamoto, Melting experiment on a model chondritic mantle composition at 25 GPa, *Geophys. Res. Lett., 14*, 733-736, 1987.

Ohtani, E., T. Kato, and H. Sawamoto, Melting of a model chondritic mantle to 20 GPa, *Nature, 322*, 352-353, 1986.

Presnall, D.C., J.R. Dixon, T.H. O'Donnell, and S.A. Dixon, Generation of mid-ocean ridge tholeiites, *J. Petrol., 20*, 3-35, 1979.

Richter, F.M., and D. McKenzie, Dynamical models for melt segregation from a deformable matrix, *J. Geol., 92*, 729-740, 1984.

Ringwood, A.E., *Origin of the Earth and Moon*, 295 pp., Springer-Verlag, New York, 1979.

Ringwood, A.E., Earliest history of the Earth-Moon system, in *Origin of the Earth*, edited by H.E. Newsom and J.H. Jones, pp. 101-134, Oxford University Press, New York, 1990.

Ringwood, A.E., T. Kato, and T. Irifune, Minor element partition relationships among high pressure minerals and implications for gross mantle differentiation (abstract), *Eos Trans. AGU, 68*, 1548, 1987.

Robie, R.A., B.S. Hemmingway, and J.R. Fisher, Thermodynamic properties of minerals and related substances at 298.15 K and 1 bar (10^5 pascals) pressure and at higher temperatures, *U.S. Geol. Surv. Bull., 142*, 1978.

Roscoe, R., Suspensions, in *Flow Properties of Disperse Systems*, edited by J.J. Hermans, pp. 1-38, North-Holland, Amsterdam, 1953.

Rumble, D., The adiabatic gradient and adiabatic compressibility, *Year Book Carnegie Inst. Washington, 75*, 651-655, 1976.

Scarfe, C.M., and E. Takahashi, Melting of garnet peridotite to 13 GPa and the early history of the upper mantle, *Nature, 322*, 354-356, 1986.

Scott, D.R., and D.J. Stevenson, Magma solitons, *Geophys. Res. Lett., 11*, 1161-1164, 1984.

Scott, D.R., and D.J. Stevenson, Magma ascent by porous flow, *J. Geophys. Res., 91*, 9283-9296, 1986.

Scott, D.R., and D.J. Stevenson, The competition between percolation and circulation in a deformable porous medium, *J. Geophys. Res., 93*, 6451-6462, 1988.

Shaw, G.H., Core formation in terrestrial planets, *Phys. Earth Planet. Inter., 20*, 42-47, 1979.

Solomon, S.C., Formation, history and energetics of cores in the terrestrial planets, *Phys. Earth Planet. Inter., 15*, 135-145, 1978.

Stacey, F.D., Thermal regime of the Earth's interior, *Nature, 255*, 44-45, 1975.

Stebbins, J.F., I.S.E. Carmichael, and L.K. Moret, Heat capacities and entropies of silicate liquids and glasses, *Contrib. Mineral. Petrol., 86*, 131-148, 1984.

Stevenson, D.J., Formation and early evolution of the Earth, in *Mantle Convection*, edited by W.R. Peltier, pp. 873-873, Gordon and Breach, New York, 1989.

Stishov, S.M., Melting at high pressures, *Sov. Phys. Usp.*, Engl. Transl., *11*, 816-830, 1969.

Stishov, S.M., Entropy, disorder, melting, *Sov. Phys. Usp.*, Engl. Transl., *31*, 52-67, 1988.

Stolper, E.M., D. Walker, B.H. Hager, and J.F. Hays, Melt segregation from partially molten source regions: The importance of melt density and source region size, *J. Geophys. Res., 86*, 6261-6271, 1981.

Takahashi, E., Melting of a dry peridotite KLB-1 up to 14 GPa: Implications on the origin of peridotitic upper mantle, *J. Geophys. Res., 91*, 9367-9382, 1986.

Takahashi, E., and C.M. Scarfe, Melting of peridotite to 14 GPa and the genesis of komatiite, *Nature, 315*, 566-568, 1985.

Thompson, C., and D.J. Stevenson, Gravitational instability in two-phase disks and the origin of the Moon, *Astrophys. J., 333*, 452-481, 1988.

Tonks, W.B., and H.J. Melosh, The physics of crystal settling and suspension in a turbulent magma ocean, in *Origin of the Earth*, edited by H.E. Newsom and J.H. Jones, pp. 151-174, Oxford University Press, New York, 1990.

Verhoogen, J., Petrological evidence on temperature distribution in the mantle of the Earth, *Eos Trans. AGU, 35*, 85-92, 1954.

Walker, D., and W.S. Kiefer, Xenolith digestion in large magma bodies, *Proc. Lunar Planet. Sci. Conf. 15th*, part 2, *J. Geophys. Res., 90*, suppl., C585-C590, 1985.

Wei, K., R.G. Tronnes, and C.M. Scarfe, Phase relations of aluminum-undepleted and aluminum-depleted komatiites at pressures of 4-12 GPa, *J. Geophys. Res., 95*, 15,817-15,827, 1990.

Zahnle, K.J., J.F. Kasting, and J.B. Pollack, Evolution of a steam atmosphere during Earth's accretion, *Icarus, 74*, 62-97, 1988.

T.J. Ahrens and E.M. Stolper, Division of Geological and Planetary Sciences, California Institute of Technology, Pasadena, CA 91125.

G.H. Miller, Department of Geology and Geophysics, University of California, Berkeley, CA 94720.

(Received March 19, 1990;
revised April 16, 1991;
accepted April 24, 1991.)